Acceleration scaling and stochastic dynamics of a fluid particle in turbulence

Rémi Zamansky

Acceleration scaling and stochastic dynamics of a fluid particle in turbulence

Rémi Zamansky[1, *]

[1] *Institut de Mécanique des Fluides de Toulouse (IMFT), Université de Toulouse, CNRS-INPT-UPS, Toulouse France*

(Dated: October 29, 2021)

It is well known that the fluid-particle acceleration is intimately related to the dissipation rate of turbulence, in line with the Kolmogorov assumptions. On the other hand, various experimental and numerical works have reported as well its dependence on the kinetic energy. In this paper, I present the statistics of the fluid-particle acceleration conditioned on both the local dissipation rate and the kinetic energy. It is shown that this quantity presents an exponential dependence on the kinetic energy, in addition to the expected power law behavior with the dissipation rate. The exponential growth, which clearly departs from the previous propositions, reflects the additive nature of the kinetic energy, and gives the possibility to see the acceleration as a multiplicative cascade process integrating the effects of sweeps by the flow structures along the fluid-particle trajectory. I then propose scaling laws for the Reynolds number dependence of the conditional and unconditional acceleration variance using the Barenblatt's incomplete similarity framework. On the basis of these observations, we introduce a vectorial stochastic model for the dynamics of a tracer in turbulent flows. This model incorporates the non-Markovian log-normal model for the dissipation rate recently proposed by Chevillard, as well as an additional hypothesis regarding non-diagonal terms in the diffusion tensor. I will show that this model is in good agreement with direct numerical simulations and presents the essential characteristics of the "Lagrangian turbulence" highlighted in recent years, namely (i) non-Gaussian PDF of acceleration, (ii) scale separation between the norm of the acceleration and its components, (iii) anomalous scaling law for the Lagrangian velocity spectra, and (iv) negative skewness of the power increments, reflecting the temporal irreversibility.

I. INTRODUCTION

With the advances of experimental techniques and the increase in computing power of the last decades, remarkable features of the dynamics of fluid particles in turbulent flows have been discovered. Among other things, the measurement of the probability distribution of the acceleration of these tracers has been shown to be very clearly non-Gaussian with a high frequency of observing very intense events [48, 60, 61, 89]. For moderate Reynolds numbers, it is relatively common to observe accelerations more than 100 times greater than its standard deviation. In addition, the components of acceleration and its norm present very different correlation times, the ratio of these characteristic times increasing with the Reynolds number [62, 63, 68] showing that the dynamics of the tracers is influenced by the full spectrum of turbulence scales. On one hand, the acceleration has been shown to be directly correlated with the local dissipation rate of turbulence [12, 36, 75, 94], in accordance with Kolmogorov's hypotheses. On the other hand, various experimental and numerical works have also reported its dependence on local kinetic energy [1, 11, 14, 24, 60, 75, 84], attributed somehow to the sweeping of small scales by large-scale flow [19, 86, 93]. The absence of proper scale separation explains that the Lagrangian correlation functions present power laws with anomalous exponents and which can be described by the multifractal formalism [2, 10, 21, 51, 82] as the signature of intermittency and persistence of viscous effects. To end this list, we mention the asymmetry of the fluctuations of the mechanical power received or given up by a fluid particle reflecting the temporal irreversibility of its dynamics [26–28, 72, 91].

Such complex phenomenology must be attributed to the collective and dissipative effects. Indeed according to the Navier-Stokes equation, the acceleration of a fluid particle is essentially given by the pressure field which is determined by all the other particles [25]. Moreover, although the Laplacian term in the Navier-Stokes equation is of order Re^{-1} smaller than the pressure gradient term, the viscosity cannot be neglected. Indeed, as a small force integrated over a long period could be significant, the viscosity insidiously affects the fluid tracer velocity. Which in turn influences the particle acceleration through modification of the pressure gradient. This is manifested by the persistence of the Reynolds number effect on the acceleration statistics, even for very large Reynolds. Such a scenario is supported by [22, 23, 66] who showed that adding noise to an inviscid Lagrangian flow leads to irreversibility of the dynamics.

Following the Kolmogorov first hypothesis [44, 46] stating that locally homogenous turbulent flows are universal, it should be possible, in principle, to propose a stochastic model that reproduces the dynamics of a single fluid particle

* remi.zamansky@imft.fr

by effectively accounting for the interactions with all the other fluid particles. Let us note that the Kolmogorov first hypothesis received some support from recent studies [15, 52, 85]. In order to propose such a stochastic model, our main assumption in this paper is to write the increments of the acceleration vector of a fluid particle as $da_i = M_i dt + D_{ij} dW_j$. Both M and D depend on the particle acceleration a and velocity u, which is simply given by the kinematic relation of a fluid particle $u_i = \int a_i dt$. It is indeed a necessary condition that a depends on u to limit the diffusion in velocity space and have statistically stationary dynamics of the fluid particle. We will propose closed expressions for M and D from basic consideration using as a starting point the acceleration statistics conditioned on both the local value of the dissipation rate and the kinetic energy observed from direct numerical simulations (DNS) and presented as well in this paper. It will be shown that introducing a "maximal winding hypothesis" associated to a non-diagonal diffusion tensor, this simple stochastic model reproduces all the statistical feature of the Lagrangian dynamics presented above without any adjustable parameter.

Let us first review some previous work on the stochastic modeling for the Lagrangian dynamics (see also [1]). Among the pioneering works, Sawford [80] proposed a scalar Gaussian model for the acceleration presenting a feedback term proportional to the velocity. Pope and Chen [71] devised a Langevin like equation for the velocity coupled with a log-normal model for the dissipation through the introduction of conditional statistics. Similarly [9, 73, 74] proposed an extension of the Sawford model leading to a non-Gaussian scalar model for the acceleration. This work was further refined by [49] who also advanced a non-Gaussian scalar model for the dynamics prescribing ad hoc shape of the conditional acceleration statistics with the dissipation along with a linear dependence on the velocity. The model introduced in [76] describes increments of the derivative of acceleration in a so-called third-order model to better account for the Reynolds number dependence on the acceleration statistics. Recently [88] proposed generalization to an infinite number of layers leading to smooth 1D trajectory along with a multifractal correction to account for intermittency, as introduced in [3, 43, 56]. An acceleration vector model has been proposed in [77] by imposing empirical correlation between velocity and acceleration, with additive noise leading to Gaussian statistics for the acceleration. Likewise, [70] presented a 3D Gaussian model, with linear dependence on the velocity as well as an extension to non-homogenous flows. In order to account for intermittency effect, in [33, 78, 97] the 3D acceleration vector is given by the product of two independent stochastic processes, one for the acceleration norm the other for its orientation, In this model the velocity feedback on the dynamics was realized by a coupling with large eddy simulation framework. To summarize, to our knowledge, a vectorial model for the tracer dynamics that is autonomous and reproducing the essential features of Lagrangian turbulence (irreversibility, non-Gausianty, multifractality) has not yet been proposed.

The essential building block of previously cited models is the conditional acceleration statistics. Previous studies have focused on conditional statistics with either the velocity or the dissipation rate separately. From the extensive analysis of [94], one can conclude that the acceleration variance conditioned on the dissipation rate ε present power law behavior for large values of ε with a Reynolds number dependent exponent.

Regarding the links between the fluid particle acceleration and their velocity, Biferale et al. [11] argue that according to the Heisenberg – Yaglom scaling for the acceleration $\langle a^2 \rangle \sim a_\eta^2 = \langle \varepsilon \rangle^{3/2} \nu^{-1/2} = \langle K \rangle^{9/4} L^{-3/2} \nu^{-1/2}$, with ν the kinematic viscosity, $K = 1/2 u_i u_i$ the kinetic energy and L the characteristic size of large structures, one should expect that the variance of the velocity-conditioned acceleration behaves like: $\langle a_n^2 | K \rangle \propto K^{9/4}$. Then on the basis of the multfractal formalism, they proposed a very close scaling law, $\langle a^2 || u | \rangle \sim |u|^{4.6}$. The proposed relation was observed to be in agreement with DNS for large velocity, typically $|u| > 3\sigma_u$ with $\sigma_u = \sqrt{2/3 \langle K \rangle}$. These events remain very rare since the PDF of the fluid velocity is Gaussian so the range of validity of the power law is, at best, very limited. On the other hand, Sawford et al. [84] propose that $\langle a_x^2 | u_x \rangle \sim u_x^6$ based on a mechanism involving vorticity tubes. This scaling law which seems compatible with the first measurements of the acceleration conditioned on velocity in [60], is confirmed neither by the DNS of [11] nor in a second experimental paper by Crawford et al. [24] which gave more credit to the $K^{9/4}$ law.

In this paper we study the acceleration statistics conditional on both the kinetic energy and the dissipation rate. To our knowledge such doubly conditional statistic of the acceleration have never been presented. It will be shown that the variance can be expressed as $\langle a^2 | \varepsilon, K \rangle \sim \exp(\alpha K / \langle K \rangle + \gamma \ln \varepsilon / \langle \varepsilon \rangle)$. This result, which is clearly in contrast with the previously proposed power law dependence on velocity, can be interpreted to propose scaling symmetry for the fluid-particle acceleration incorporating effects of sweeps. We also propose to apply the incomplete similarity framework introduced by Barenblatt to account for Reynolds number dependence and intermittency correction. That enables to provide as well new scaling relations for the unconditional variance in good agreement with the DNS. Eventually the doubly conditional statistic of the acceleration which gives a relation between the force, the energy and the power will serve as corner stone to build the stochastic model for the dynamics of a fluid particle mentioned above.

In section II we present the statistic of the acceleration conditioned on the local value of the dissipation rate and kinetic energy obtained from DNS. Then we show that the Reynolds number dependence on the acceleration conditioned on the dissipation rate can be described using the Barenblatt incomplete similarity. We deduce a new

relation for the unconditional acceleration variances. To end this section, we show that these new results can be interpreted as a multiplicative cascade for the acceleration with scale dependent sweeping effect. Then in section III we give the derivation of the stochastic model for the single fluid particle dynamics taking as an initial step the doubly conditional acceleration variance, and present the outcome of the model for the Reynolds number up to $Re_\lambda = 9000$ along with comparison with DNS results when available.

II. SCALING LAWS OF THE ACCELERATION

A. Methodology

We present in this section results concerning the statistics of the acceleration of a fluid particle. These results have been obtained from direct numerical simulations (DNS) of isotropic turbulence in a periodic box at a Taylor-scale Reynolds number of $Re_\lambda = 250$. We used pseudo-spectral code as detailed in [53, 95, 97]. The DNS was carried out at a resolution of 1024^3, with the large scale forcing proposed by [47]. The statistics are computed from 40 3D-fields sampled at roughly each eddy-turnover time.

We will show statistics of the acceleration conditioned by the dissipation rate and the kinetic energy. Note that in this paper we consider the pseudo-dissipation $\tilde{\varepsilon} = \nu(\partial_j u_i)^2$, which is the second invariant of the velocity gradient tensor multiply by the viscosity rather than the dissipation $\varepsilon = \frac{1}{2}\nu(\partial_j u_i + \partial_i u_j)^2$. We prefer to show here the statistics of the pseudo-dissipation to be consistent with the next section of the paper, in which we will use the log-normal distribution hypothesis for the dissipation. Indeed, this property is very well verified for the pseudo-dissipation whereas it is only approximate for the dissipation [94]. Nevertheless, the statistics presented below have also been computed considering the dissipation, ε, and no significant differences were observed. To lighten the paper, in the sequel, we will drop the tilde in the notation of the pseudo-dissipation, as well, in the text, we will write dissipation instead of pseudo-dissipation.

B. Conditional statistics given the dissipation and the kinetic energy

In order to illustrate the relationships between acceleration, energy dissipation and kinetic energy, we show in Fig. 1 visualizations of these quantities at the same instant obtained from our DNS. We notice that $\log a^2/\langle a^2\rangle$ and $\log \varepsilon/\langle\varepsilon\rangle$ show a fairly marked correlation. In addition, it seems that some areas of the flow where the kinetic energy is high also correspond to regions of high acceleration magnitude.

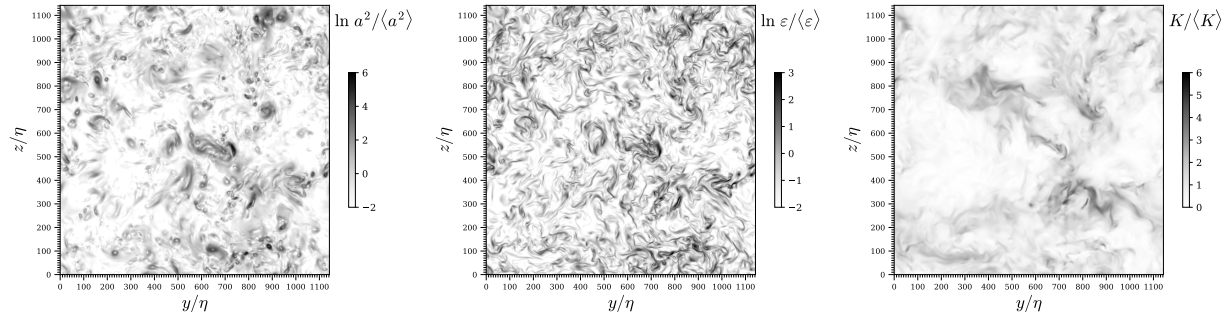

FIG. 1. Visualization of the instantaneous fields of the square of the acceleration, of the dissipation and of the kinetic energy in a cut $y - z$ of the flow by DNS at $Re_\lambda = 250$. (a): $\ln(a^2/ < a^2 >)$; (b): $\ln(\varepsilon/ < \varepsilon >)$ and (c): $K/ < K >$.

Figure 2 presents the variance of the acceleration of a fluid particle conditioned to the local value of the kinetic energy and the dissipation rate: $\langle a^2|\varepsilon, K\rangle$. In Fig. 2 (a), the levels of the logarithm of the conditional variance are shown as a function of K and of ε. We see that the conditional variance of the acceleration depends on these two quantities and that the dependence on K seems somewhat similar to that of $\ln \varepsilon$. In a more quantitative way, we show in Fig. 2 (b) the variance of the acceleration as a function of ε for different values of K. We can see that the shape of the curves remains globally unchanged when K varies and also presents the same shape as the variance conditioned by ε only as also presented in this figure. Essentially, it is observed that the conditional variance presents power law behavior for $\varepsilon \gg \langle\varepsilon\rangle$ with an exponent close to 3/2. As discussed in more details below, we observe a slight deviation of the scaling law compared to the acceleration conditioned only by the dissipation.

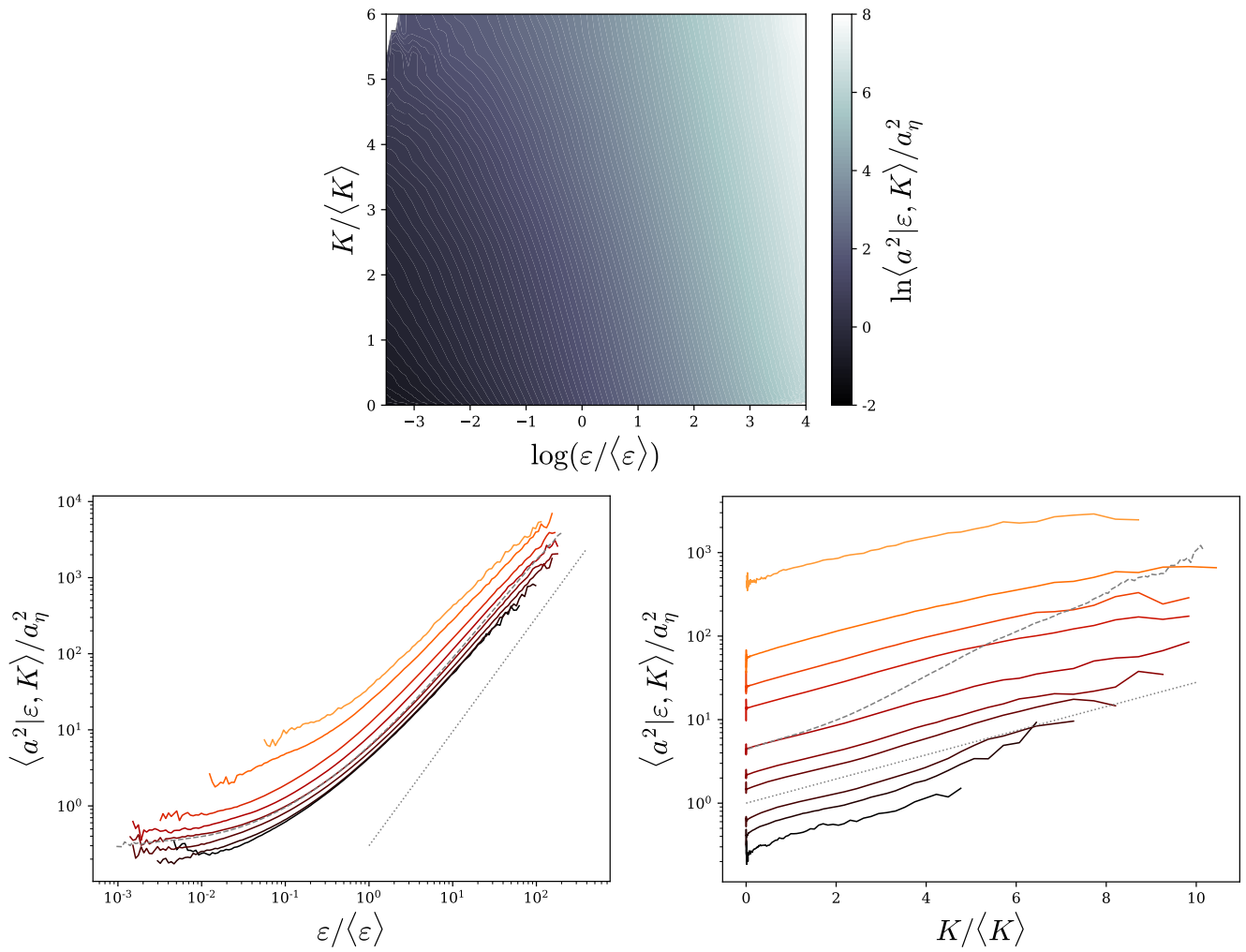

FIG. 2. Variance of acceleration conditioned on the local dissipation rate and kinetic energy obtained from DNS at $Re_\lambda = 250$. (a) Map of $\log\langle \boldsymbol{a}^2|\varepsilon, K\rangle/\langle \boldsymbol{a}^2\rangle$ versus $\log \varepsilon/\langle\varepsilon\rangle$ and $K/\langle K\rangle$. (b) Plot, in logarithmic scales, of $\langle \boldsymbol{a}^2|\varepsilon, K\rangle/a_\eta^2$ against $\varepsilon/\langle\varepsilon\rangle$ for $K/\langle K\rangle = 0.025, 0.1, 0.5, 1, 2, 3, 5, 6.5 \pm 30\%$ from black to orange. Comparison with $\langle \boldsymbol{a}^2|\varepsilon\rangle/a_\eta^2$ in gray dashed line and with the power law $(\varepsilon/\langle\varepsilon\rangle)^{3/2}$ in gray dotted line. (c) Plot, in semi-logarithmic scales, of $\langle \boldsymbol{a}^2|\varepsilon, K\rangle/a_\eta^2$ against $K/\langle K\rangle$ for $\varepsilon/\langle\varepsilon\rangle = 0.01, 0.05, 0.1, 0.3, 0.5, 1, 3, 5, 10, 50 \pm 30\%$ from black to orange. Comparison with $\langle \boldsymbol{a}^2|K\rangle/a_\eta^2$ in gray dashed line and with $\exp(\alpha K/\langle K\rangle)$ with $\alpha = 1/3$ in gray dotted line.

Figure 2 (c) shows the variance of the acceleration as a function of K for different values of ε. As expected, we find that the variance of the acceleration increases with K. We clearly notice an exponential growth of the variance over the whole range of K with a growth rate α which appears independent of ε:

$$\langle a^2|\varepsilon, K\rangle = c_\varepsilon a_\eta^2 \exp(\alpha K/\langle K\rangle) \tag{1}$$

with $a_\eta^2 = \langle\varepsilon\rangle^{3/2}\nu^{-1/2} = \langle\varepsilon\rangle/\tau_\eta$ the so-called Kolmogorov acceleration and the prefactor c_ε depending on ε. From our DNS it appears that $\alpha \approx 1/3$. Note that we find the same value of α from the database of [8, 50] obtained for $Re_\lambda = 400$ suggesting that the value of α is independent of the Reynolds number. We do not show these results, because the statistical convergence is not ideal.

This exponential behavior contrasts with the references mentioned in the introduction in which power laws behavior for the variance conditioned on K solely had been proposed. Nevertheless, we can notice that exponential growth does not seem to disagree with the data presented in these references. Interestingly, this relationship only depends on a characteristic velocity, not time or length scale separately. The absence of characteristic time is attributed to the scale separation between large structures and small ones, such that the large structures of the flows appear as quasi stationary and infinite to the smallest one and only their velocity matters.

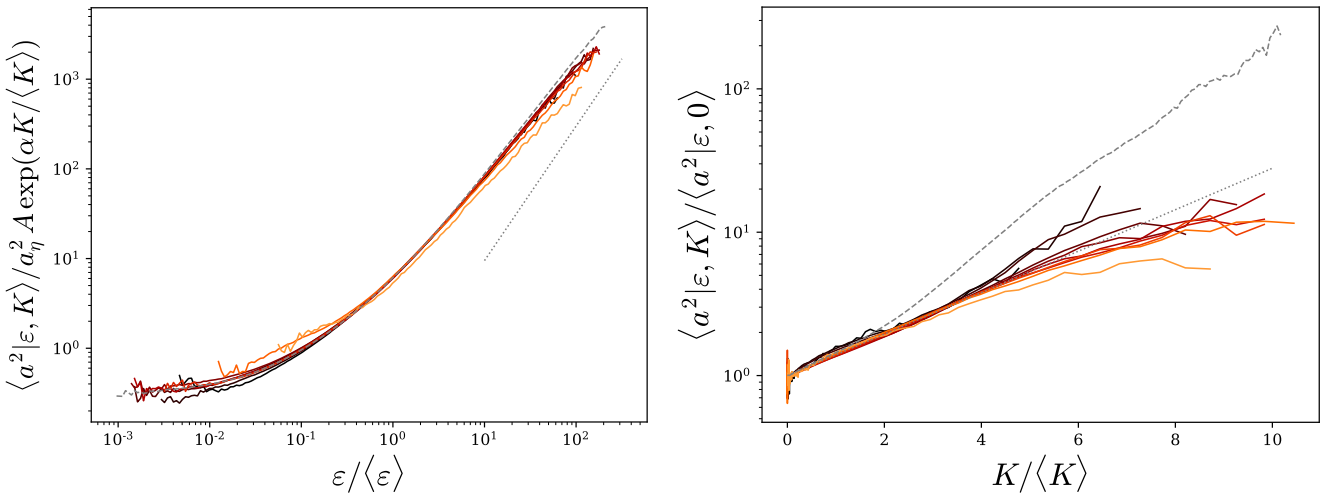

FIG. 3. Normalized Variance of acceleration conditioned on the local dissipation rate and kinetic energy obtained from DNS at $Re_\lambda = 250$. (a) Plot of $\langle a^2|\varepsilon, K\rangle / A a_\eta^2 \exp(\alpha K/\langle K\rangle)$ against $\varepsilon/\langle\varepsilon\rangle$ for various values of K. Comparison with $\langle \boldsymbol{a}^2|\varepsilon\rangle / a_\eta^2$ in gray dashed line and with the power law $(\varepsilon/\langle\varepsilon\rangle)^{3/2}$ in gray dotted line. (b) Plot of $\langle a^2|\varepsilon, K\rangle / \langle a^2|\varepsilon, K=0\rangle$ against $K/\langle K\rangle$ for various values of $\varepsilon/\langle\varepsilon\rangle$. Comparison with $\langle \boldsymbol{a}^2|K\rangle / a_\eta^2$ in gray dashed line and with $\exp(\alpha K/\langle K\rangle)$ with $\alpha = 1/3$ in gray dotted line The ranges for the fixed values of K and ε for both plots are the same as in Fig. 2.

In appendix A we show that assuming that the fluctuations of the kinetic energy are independent of the fluctuations of the dissipation rate and that the velocity components of a fluid particle are Gaussian and independent, one can estimate the factor c_ε as :

$$c_\varepsilon \approx A \langle a^2|\varepsilon\rangle / a_\eta^2 \tag{2}$$

where $A = \left(1 - \frac{2}{3}\alpha\right)^{3/2}$, which is equal to $A = 7\sqrt{7}/27 \approx 0.686$, for $\alpha = 1/3$, neglecting the small logarithmic dependence on $\varepsilon/\langle\varepsilon\rangle$.

Consequently, for large Reynolds numbers, the doubly conditioned variance of the fluid-particle acceleration is expressed as

$$\langle a^2|\varepsilon, K\rangle = A \langle a^2|\varepsilon\rangle \exp(\alpha K/\langle K\rangle) \tag{3}$$

This relation is confirmed in Fig. 3 which presents the conditional variance of the acceleration normalized by $A a_\eta^2 \exp(\alpha K/\langle K\rangle)$ as a function of ε for different values of K as well as normalized by $A\langle a^2|\varepsilon\rangle = \langle a^2|\varepsilon, K=0\rangle$ as a function of K for different values of ε. It can be seen that a fairly good overlap of the various curves is obtained, confirming the self-preserving character of the acceleration conditioned on both the kinetic energy and the dissipation rate.

C. Similarity of the conditional statistics given the dissipation

We propose now to focus with more details on the scaling law of the acceleration variance conditioned on the dissipation rate only $\langle a^2|\varepsilon\rangle$. For that we consider the DNS data from Yeung et al. [94], along with our DNS data. Figure 4(a) presents the conditional acceleration variance for Reynolds numbers in the range $Re_\lambda = 40$ to 680. We first notice that for weak values of the dissipation rate ($\varepsilon \ll \langle\varepsilon\rangle$) the value of the conditional acceleration variance tends towards an asymptotic value, which depends on the Reynolds number. The saturation of the conditional acceleration can be attributed to the effect of the sweeping by the large structures of the flow which dominates in low dissipative regions. We denote by a_0^2 the asymptotic value of the conditional variance:

$$a_0^2 = \lim_{\varepsilon \to 0} \langle a^2|\varepsilon\rangle \tag{4}$$

Assuming that the acceleration of fluid particles in low dissipative regions is mainly influenced by large scales, we can estimate a_0^2 as $a_0^2 \sim \langle K\rangle/\tau_L^2$ with τ_L the integral time scale of the flow. This leads to the following estimate:

$$a_0^2/a_\eta^2 \sim \tau_\eta/\tau_L \sim Re_\lambda^{-1} \tag{5}$$

We test this scaling law for a_0 in Fig. 4(b) by presenting a_η^2/a_0^2 as a function of Re_λ from the different DNS datasets. We observe a linear growth rate of a_0^2/a_η^2 with $1/Re_\lambda$. More specifically, from the DNS we estimate $a_0^2/a_\eta^2 \approx (0.005Re_\lambda + 1.5)^{-1}$.

For large values of ε, we notice in Fig. 4(a), as already reported in [94], that the conditional variance presents a power law behavior with ε. However, the exponent of this scaling law is seen to evolve continuously with the Reynolds number, and seems to tend asymptotically towards $\varepsilon^{3/2}$. By dimensional analysis we can define f as:

$$\frac{\langle a^2|\varepsilon\rangle}{\varepsilon^{3/2}\nu^{-1/2}} = f(\varepsilon/\langle\varepsilon\rangle, Re_\lambda) \tag{6}$$

In the inset of Fig. 4(a), it is seen that f seems to admit an asymptotic constant value for $\varepsilon \gg \langle\varepsilon\rangle$ only in the limit of very large Reynolds number. This is reminiscent of the incomplete similarity framework proposed by Barenblatt [4–6]. Following Barenblatt, we assume that f presents an incomplete similarity in $\varepsilon/\langle\varepsilon\rangle$ and absence of similarity in Re_λ. Accordingly we write

$$f(\varepsilon/\langle\varepsilon\rangle, Re_\lambda) = B\,(\varepsilon/\langle\varepsilon\rangle)^\beta \tag{7}$$

where the anomalous exponent β, and the prefactor B are both functions of Re_λ. Arguing for a vanishing viscosity principle, Barenblatt further proposed that the critical exponent presents inverse logarithmic dependence on Re_λ, which is also in agreement with the log-similarity proposed by [18, 29]. Expending β and B in power of $1/\ln(Re_\lambda)$ yields, keeping only the leading-order term in Re_λ:

$$\beta = \beta_0 + \beta_1/\ln Re_\lambda \tag{8}$$

$$B = B_0 + B_1/\ln Re_\lambda \tag{9}$$

To have a finite limit, consistently with the vanishing viscosity principle we have $\beta_0 = 0$. The remaining constants B_0, B_1 and β_1 are then determined by comparison with the DNS data. From the inset of Fig. 4(a) we see that both β and B are increasing function of Re_λ. In Fig. 5(a) we assess the relation (7)-(9) by plotting $\chi = \dfrac{1}{3/2+\beta}\ln(1/B\,\langle a^2|\varepsilon\rangle/a_\eta^2)$ against $\ln(\varepsilon/\langle\varepsilon\rangle)$ for various Reynolds numbers. It is observed that with $B_0 = 5.8$, $B_1 = -20$ and $\beta_1 = -4/3$, all the DNS data collapse on the line $\chi = \ln(\varepsilon/\langle\varepsilon\rangle)$ (the bisectrix of the graph) for $\varepsilon \gg \langle\varepsilon\rangle$, validating the scaling relation.

We can go a step further by introducing χ_0 as $\chi_0 = \lim_{\varepsilon\to 0}\chi = \dfrac{1}{3/2+\beta}\ln(1/B\,a_0^2/a_\eta^2)$. Then, evidently $\chi - \chi_0 = \ln\left(\langle a^2|\varepsilon\rangle/a_0^2\right)^{1/(3/2+\beta)}$ would give 1 in the low dissipative regions ($\varepsilon \ll \langle\varepsilon\rangle$) and for $\varepsilon \gg \langle\varepsilon\rangle$, $\chi - \chi_0$ should collapse on

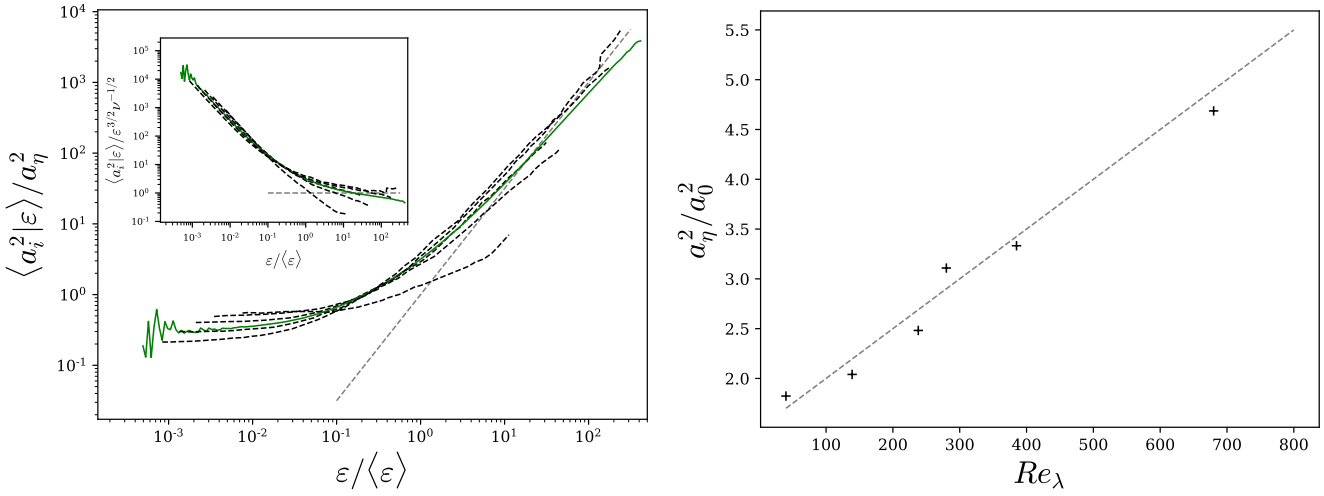

FIG. 4. (Left) Acceleration variance conditioned on the local dissipation rate normalized by the Kolmogorov acceleration $\langle \boldsymbol{a}^2|\varepsilon\rangle/a_\eta^2$. The dashed lines correspond to the DNS of Yeung et al. [94] for $Re_\lambda = 40, 139, 238, 385, 680$, the green continuous line is for our DNS at $Re_\lambda = 250$. Comparison with the power law $(\varepsilon/\langle\varepsilon\rangle)^{3/2}$. Inset conditional acceleration normalized by $\varepsilon^{3/2}\nu^{-1/2}$. (Right) a_η^2/a_0^2 as a function of Re_λ with $a_0^2 = \lim_{\varepsilon\to 0}\langle a_i^2|\varepsilon\rangle/a_\eta^2$ the acceleration variance in low dissipative regions. Comparison with the line $0.005Re_\lambda + 1.5$ in dashed line.

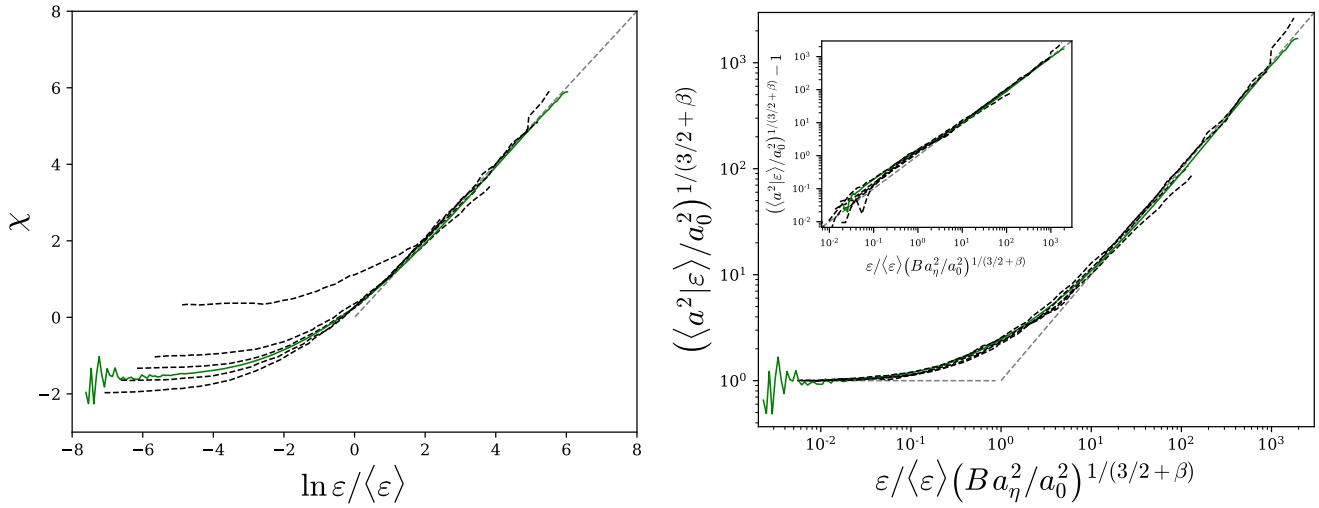

FIG. 5. (Left) Evolution of $\chi = \dfrac{1}{3/2+\beta}\ln(1/B\,\langle a^2|\varepsilon\rangle/a_\eta^2)$ versus $\ln\varepsilon/\langle\varepsilon\rangle$ with $B = B_0 + B_1/\ln(Re_\lambda)$ and $\beta = \beta_1/\ln(Re_\lambda)$ and $B_0 = 5.8$, $B_1 = -20$ and $\beta_1 = -4/3$, for various Re_λ: dashed lines for the DNS of Yeung et al. [94] for $Re_\lambda = 139, 238, 385, 680$, and green continuous line for our DNS at $Re_\lambda = 250$. Comparison with the line $\chi = \ln\varepsilon/\langle\varepsilon\rangle$ in gray dashed line. (Right) Evolution of $\left(\langle a^2|\varepsilon\rangle/a_0^2\right)^{1/(3/2+\beta)}$ against $\varepsilon/\langle\varepsilon\rangle\left(Ba_\eta^2/a_0^2\right)^{1/(3/2+\beta)}$ for the various Reynolds number. Inset: plot of $\left(\langle a^2|\varepsilon\rangle/a_0^2\right)^{1/(3/2+\beta)} - 1$ against $\varepsilon/\langle\varepsilon\rangle\left(Ba_\eta^2/a_0^2\right)^{1/(3/2+\beta)}$.

in the line $\ln(\varepsilon/\langle\varepsilon\rangle) - \chi_0 = \ln\left[\varepsilon/\langle\varepsilon\rangle\left(Ba_\eta^2/a_0^2\right)^{1/(3/2+\beta)}\right] = \ln\zeta$. This is seen in Fig. 5(b) that presents the evolution of $\left(\langle a^2|\varepsilon\rangle/a_0^2\right)^{1/(3/2+\beta)}$ against ζ for the various Reynolds numbers considered here.

Moreover it is interesting to note that the curves are all overlapping even for intermediate values of ε, suggesting that the conditional acceleration variance can be cast in a self-similar form:

$$\langle a^2|\varepsilon\rangle = a_0^2\left(\phi(\zeta)\right)^{3/2+\beta} \tag{10}$$

with ϕ a universal function of only one argument $\phi = \phi(\zeta)$ with the asymptotics $\phi(\zeta) = 1$ for $\zeta \ll 1$ and $\phi(\zeta) = \zeta$ for $\zeta \gg 1$. Making a Taylor expansion of ϕ around $\zeta = 0$ and using a matching asymptotic argument, simply yields to $\phi(\zeta) = 1 + \zeta$. It is seen in the inset of the Fig. 5(b) that the proposed expression for ϕ gives a good approximation of the data over the whole range of ε. We can indeed observe more than 5 decades of quasi-linear growth of $\chi - \chi_0 - 1$ with ζ.

The non-dimensional function f introduced in (6) can, in consequence, be express as:

$$f(\varepsilon/\langle\varepsilon\rangle, Re_\lambda) = B\left(\varepsilon/\langle\varepsilon\rangle\right)^\beta\left(1+\frac{1}{\zeta}\right)^{3/2+\beta} \tag{11}$$

where the term within the brackets is interpreted as a correction factor for small dissipative regions. Accordingly, we obtain the following expression for the conditional acceleration variance:

$$\langle a^2|\varepsilon\rangle = Ba_\eta^2\left(\left(\frac{1}{B}\frac{a_0^2}{a_\eta^2}\right)^{1/(3/2+\beta)} + \frac{\varepsilon}{\langle\varepsilon\rangle}\right)^{3/2+\beta} \tag{12}$$

As the parameters β and B are slowly evolving functions of Re_λ, the expressions for β and B remain speculative since their proper validation would require a much larger range of Reynolds numbers.

D. Reynolds number dependence of the unconditional acceleration variance

Assuming the distribution of dissipation, we can integrate relation (12) to obtain the unconditional variance $\langle a^2\rangle = \int\langle a^2|\varepsilon\rangle P(\varepsilon)d\varepsilon$ and thus propose an alternative formula to the empirical relation proposed in [35, 84, 94]. We consider that $\varepsilon/\langle\varepsilon\rangle$ presents a log-normal distribution with parameter $\sigma^2 \approx 3/8\ln Re_\lambda/R_c$ with $R_c = 10$ as shown by [94] from

DNS data, consistently with the proposition of Kolmogorov and Oboukhov [46, 64]. Notice nevertheless that other expressions for σ^2 have been proposed in the literature reflecting the vanishing viscosity limits [5, 17]. Taking for $\langle a^2|\varepsilon\rangle$ the expression (12) we perform the integration numerically with the expression (8) and (9) for β and B with the values of B_0, B_1 and β_1 and the expression of a_0^2/a_η^2 proposed above. The resulting evolution of the acceleration variance with the Reynolds number is presented in Fig. 9. It is seen that the predicted acceleration variance is in very good agreement with the DNS of [94] and is also very close to the relation proposed by [84]. The first term in brackets in (12) is the footprint of the large-scale structures whose effects is vanishing as soon as the local dissipation rate is larger than $\varepsilon/\langle\varepsilon\rangle > (B\, a_\eta^2/a_0^2)^{-1/(3/2+\beta)}$ and therefore can be neglected when the Reynolds number is large since $a_0^2/a_\eta^2 \sim 1/Re_\lambda$. In consequence for large Reynolds numbers, equation (12) reduces to:

$$\langle a^2|\varepsilon\rangle/a_\eta^2 = B\left(\frac{\varepsilon}{\langle\varepsilon\rangle}\right)^{3/2+\beta} \tag{13}$$

With this expression the acceleration variance is simply estimated from the moments of the log-normal distribution as:

$$\frac{\langle a^2\rangle}{a_\eta^2} = B\,(Re_\lambda/R_c)^{9/64+3\beta/8(1+\beta/2)} \tag{14}$$

This expression is also presented in Fig. 9 and is shown to converge to the previous estimate as the Reynolds number increases. At $Re_\lambda \approx 100$ the two estimates for the variance differ by about 40% while there is about 15% of difference at $Re_\lambda \approx 500$. Confirming that the a_0^2 term is indeed vanishing at large Reynolds numbers. Both expression tends asymptotically to the power law:

$$\langle a^2\rangle/a_\eta^2 = 2.54 B_0 Re_\lambda^{9/64} \tag{15}$$

where we have used (8) to write $R_c^{-9/64} B0 \exp(3\beta_1/8) \approx 2.54$ This expression is presented as well in Fig. 9, confirming that the convergence to the power law is very slow.

E. Multiplicative cascade for the acceleration

Substituting (13) into (3), we can eventually estimate the doubly conditional acceleration variance for large Reynolds numbers as:

$$\langle a^2|\varepsilon, K\rangle/a_\eta^2 = C\exp(\alpha K/\langle K\rangle)\left(\frac{\varepsilon}{\langle\varepsilon\rangle}\right)^{\gamma} \tag{16}$$

where $C = A\,B$ with parameters A and B have been determined above and $\gamma = 3/2 + \beta$.

We complete the statistical description of the conditional acceleration by showing in Fig. 6, its probability density function (PDF). In this figure we compare the PDF of the acceleration conditional on the dissipation and the kinetic energy, with the PDF conditioned only by the dissipation and with the unconditional PDF obtained from our DNS at $Re_\lambda = 250$. All the PDFs are normalized by their respective standard deviation. It is observed that the conditional PDFs present much less developed tails than the unconditional PDF. Moreover the doubly conditional PDFs overlap with the simply conditional PDF, showing that conditioning by the velocity does not alter the shape of the PDF. As well the shape is observed to be invariant for all values of ε, supporting the idea of a canonical distribution presented in [16].

We end this section by discussing a multiplicative cascade model for the acceleration incorporating sweeping effects. Fluctuations of the locally-space-averaged dissipation rate can be modeled by multiplicative cascades [45, 59, 92]. Such model proposes to express the local dissipation over a volume of size $\ell = L\lambda^N$, with $\lambda < 1$ and L being the large scale of the flow, as the product of N random numbers:

$$\varepsilon_\ell = \langle\varepsilon\rangle \prod_{i=1}^{N} \xi_i \tag{17}$$

For N large, this yields log-normal distribution of ε_ℓ assuming the ξ_i are independent and identically distributed (and have as well finite variance). We propose likewise to write the squared acceleration, coarse-grained at scale ℓ, as :

$$a_\ell^2 = a_0^2 \prod_{i=1}^{N} \theta_i \tag{18}$$

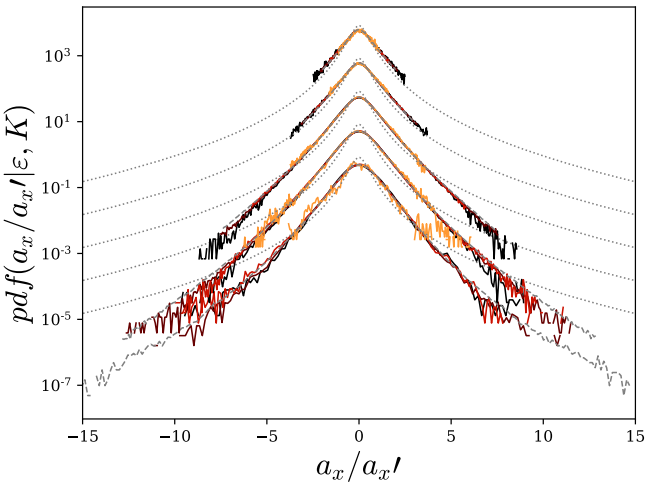

FIG. 6. PDF of the acceleration conditional on the dissipation and the kinetic energy $P(a_i|\varepsilon, K)$ for various values of ε and K: $K/\langle K\rangle = 0.1$, 1, 2.5 and 5 ± 30 from black to orange respectively and $\varepsilon/\langle\varepsilon\rangle = 0.05$, 0.3, 1, 5 and $10 \pm 30\%$ shifted respectively by one decade upward. Comparison with the acceleration PDF conditioned only by the dissipation in gray dashed line, and with the unconditional PDF in dotted gray line. Each PDF is normalized by its standard deviation. Data from our DNS at $Re_\lambda = 250$.

The scale-to-scale transformation factor θ_i is given by:

$$\theta_i = k \exp\left(\frac{\alpha}{\langle K\rangle}\frac{1}{2}u_i^2\right)(\xi_i)^\gamma = k \exp\left(\frac{\alpha}{\langle K\rangle}\frac{1}{2}u_i^2 + \gamma \ln \xi_i\right) \tag{19}$$

where u_i is the velocity of eddies of size $L\lambda^i$, which is also a fluctuating quantity. The exponential modulation is then interpreted as the sweeping effect due to these structures.

With this expression we obtain for a_ℓ^2:

$$a_\ell^2 = a_0^2 k^N \exp\left(\frac{\alpha}{\langle K\rangle}\sum_{i=1}^{N}\frac{1}{2}u_i^2 + \gamma\sum_{i=1}^{N}\ln\xi_i\right) \tag{20}$$

Setting $N = \ln(\eta/L)/\ln(\lambda) \sim \ln Re_\lambda$, η being the Kolmogorov length scales we have $K = \sum_{i=1}^{N}\frac{1}{2}u_i^2$ due to the additive nature of the kinetic energy. Thereby with $k = (C\, a_\eta^2/a_0^2)^{1/N}$ and using (17), we obtain back (16) by taking the conditional average of (20). The order of magnitude of the eddy velocities can be estimated from the Kolmogorov relation $(\varepsilon_\ell \ell)^{1/3}$ showing that a priori the sum is dominated by the large scales but, on the other hand, because of the intermittent behavior of ε_ℓ it may well happen that sweeping by small-scale structures can be dynamically important as discussed in [19].

The dissipation presents large fluctuations leading to very important accelerations and therefore to a local increase of the velocity. When the kinetic energy becomes significantly larger than on average, then the modulation of the acceleration by the exponential term becomes preponderant, thus offering a feedback mechanism allowing obtaining normal fluctuations of the velocity. This dynamic scenario involving a "self induce sweeping" which is only presented qualitatively here, is developed in the next section. Note nevertheless that it appears consistent with the recent DNS analysis of [67] showing that the particles undergo energy gains in intense dissipative regions.

III. STOCHASTIC MODELING OF THE FLUID-TRACER DYNAMICS

A. Model formulation

The foregoing multiplicative model suggests that the acceleration norm can be determined from the local kinetic energy and dissipation rate:

$$a^2 = f(K, \varepsilon) = a_\eta^2 C \left(\frac{\varepsilon}{\langle\varepsilon\rangle}\right)^\gamma \exp\left(\alpha\frac{K}{\langle K\rangle}\right) \tag{21}$$

Both K and ε are considered as stochastic variables reflecting the very large number of degrees of freedom that control them.

Considering that the increments of ε are independent of those of K, owing to the scale separation assumption in large Reynolds number flows, we express the increments of a^2 with a second order Taylor expansion in dK and $d\varepsilon$ as:

$$da^2 = a^2 \left(\alpha \frac{dK}{\langle K \rangle} + \gamma \frac{d\varepsilon}{\varepsilon} + \frac{\alpha^2}{2} \frac{dK^2}{\langle K \rangle^2} + \frac{\gamma(\gamma-1)}{2} \frac{d\varepsilon^2}{\varepsilon^2} + \gamma\alpha \frac{dK}{\langle K \rangle} \frac{d\varepsilon}{\varepsilon} \right) \tag{22}$$

We consider in a fairly general way that the dissipation ε follows a multiplicative stochastic process:

$$d\varepsilon = \varepsilon \Pi dt + \varepsilon \Sigma dW \tag{23}$$

where dW are the increments of the Wiener process ($\langle dW \rangle = 0$; $\langle dW^2 \rangle = dt$). We specify the terms Π and Σ below. Substituting (23) into (22) one obtains, at first order in dt following the Ito calculus:

$$da^2 = a^2 \left[\frac{\alpha}{\langle K \rangle} P + \gamma \Pi + \frac{\gamma(\gamma-1)}{2} \Sigma^2 \right] dt + \gamma a^2 \Sigma dW \tag{24}$$

We used the identity $dK = u_i du_i = u_i a_i dt = P dt$ where P is the mechanical power per unit of mass exchanged by the fluid particle. Clearly even when Π and Σ are known (24) is not closed, as it remains to estimate $P = a_i u_i$ which requires knowing a_i and u_i.

We introduce a vectorial stochastic model for the dynamics of a fluid particle. We are looking for a stochastic process of the form:

$$du_i = a_i dt \tag{25}$$

$$da_i = M_i dt + D_{ij} dW_j \tag{26}$$

with dW_j the increments of the jth component of a tridimensional Wiener process ($\langle dW_j \rangle = 0$; $\langle dW_i dW_j \rangle = dt \delta_{ij}$). A priori the vector $\boldsymbol{M}$ and the tensor $\boldsymbol{D}$ depend on the vectors $\boldsymbol{a}$ and $\boldsymbol{u} = \int \boldsymbol{a} dt$. Indeed, $\boldsymbol{M}$ must depend on $\boldsymbol{u}$ to allow the particle velocity to reach a statistically steady state.

We will now propose expressions for M_i and D_{ij}. For this, we want to impose, on the one hand, that the model is isotropic ($\langle a_i a_j \rangle = 0$ for $i \neq j$) and that its norm $a^2 = a_i a_i$ is compatible with the expression (24). We therefore write the stochastic equation for $a_{ij}^2 = a_i a_j$ deriving from (26), thanks to the Ito formula:

$$\begin{aligned} da_{ij}^2 &= a_j da_i + a_i da_j + da_i da_j \\ &= \left(M_i a_j + M_j a_i + D_{ik} D_{jk} \right) dt + \left(a_j D_{ik} + a_i D_{jk} \right) dW_k \end{aligned} \tag{27}$$

For the square of the norm $a^2 = a_i a_i$, we have:

$$da^2 = \left(2 a_i M_i + D_{ij} D_{ij} \right) dt + 2 a_i D_{ij} dW_j \tag{28}$$

We will then proceed by identification between (28) and (24). We proceed in a similar way as [31] and [65] by identifying first the square of the diffusion term and then the drift term.

1. *Identification of the diffusion term and maximum winding hypothesis*

Quite generally, we can decompose the diffusion tensor into:

$$D_{ij} = c_1 \delta_{ij} + S_{ij} + \Omega_{ij} \tag{29}$$

where S_{ij} is a zero-trace symmetric tensor and Ω_{ij} is an antisymmetric tensor. The latter can be written as $\Omega_{ij} = \epsilon_{ijk} \omega_k$ with ϵ_{ijk} the Levi-Civita permutation symbol and ω_k a pseudo-vector. S_{ij} must be zero in order to guarantee the statistical isotropy of the acceleration. However, Ω_{ij} can be different from 0. Indeed, the experimental results of [61] and numerical results of [68] have shown that the acceleration presents scale separation between the evolution of the components and its norm, and that this separation can be introduced in modeling the evolution of the norm and orientation vector [33, 79, 96]. Stochastic model for orientation can be formulated as diffusion process with a rotational part in the diffusion tensor [33, 90]. The model for the dynamics (25) - (26) involving only two vectors $\boldsymbol{a}$ and $\boldsymbol{u}$ we propose to form the pseudo-vector $\boldsymbol{\omega}$ from these two vectors in order to keep a closed model: $\omega_k = c_2 \epsilon_{klm} a_l u_m$.

The model remains statistically isotropic and the chirality of the flow is not broken neither since the odd moments of dW_j are zero (Gaussian with zero mean). In other words the sign of c_2 has no importance. We then have:

$$D_{ij} = c_1\delta_{ij} + c_2(a_i u_j - a_j u_i) \tag{30}$$

It is to note that c_1 and c_2 are not constant, as we will see shortly.

By identifying the square of the diffusion term in (24) and (28) we find:

$$\gamma^2(a^2)^2\Sigma^2 = 4a_i a_j D_{ik} D_{jk} \tag{31}$$

Expanding with the proposed expression (30) we find:

$$\gamma^2(a^2)^2\Sigma^2 = 4a^2(c_1^2 + c_2^2(2a^2K - P^2)) \tag{32}$$

Which gives for c_1:

$$c_1^2 = \frac{\gamma^2}{4}a^2\Sigma^2 - c_2^2(2a^2K - P^2) = a^2\left(\frac{\gamma^2}{4}\Sigma^2 - 2c_2^2K\left(1 - \frac{a_T^2}{a^2}\right)\right) \tag{33}$$

where we have introduced the tangential acceleration a_T, as the projection of the acceleration vector in the direction of the velocity vector: $a_T = a_i u_i/\sqrt{u^2} = P/\sqrt{2K}$. The equation (33) imposes a constraint on c_2 in order to guarantee the positivity of c_1^2:

$$c_2^2 2K < \frac{\gamma^2}{4}\Sigma^2 \tag{34}$$

since $0 \geq 1 - \dfrac{a_T^2}{a^2} \geq 1$. So in order to guarantee the positivity of c_1^2 whatever K we conclude that c_2^2 must be proportional to $1/K$. We then introduce the parameter c_R as $c_2^2 = \dfrac{\gamma^2}{4}\Sigma^2\dfrac{c_R^2}{2K}$ with the constraint $c_R^2 \leq 1$. This gives for c_1:

$$c_1^2 = \frac{\gamma^2}{4}\Sigma^2\left(a^2(1 - c_R^2) + c_R^2 a_T^2\right) \tag{35}$$

Subsequently, we will only consider the limit $c_R = 1$ corresponding to the maximum rotational part of the diffusion tensor. We will discuss this choice in more detail below in section III C, when presenting the results.

Finally, from (30), and the expressions of c_1 and c_2, we write the components of the diffusion tensor as

$$D_{ij} = \sqrt{\frac{\gamma^2}{4}\Sigma^2}\left[\sqrt{a_T^2}\delta_{ij} + \sqrt{a_N^2}\epsilon_{ijk}b_k\right] \tag{36}$$

where we introduced a_N the normal component of the acceleration: $a_N^2 = a^2 - a_T^2$ and b_k the bi-normal unit vector[1]: $b_k = \epsilon_{klm}u_l a_m/|\epsilon_{hij}u_i a_j|$.

Note that b_k, a_T and a_N are not well defined when $K = 0$. However, when $K = 0$ we must have $c_2 = 0$ and we will therefore consider $c_R = 0$.

2. Determination of the drift term

Identifying the drift term between (28) and (24) we get:

$$2a_i M_i + D_{ij}D_{ij} = a^2\left(\frac{\alpha}{\langle K\rangle}P + \gamma\Pi + \frac{\gamma(\gamma-1)}{2}\Sigma^2\right) \tag{37}$$

---

[1] To obtain this relation we notice that $a_i u_j - a_j u_i = \epsilon_{ijk}\epsilon_{klm}a_l u_m$ and that the vector b_k is the unit vector collinear to $\epsilon_{klm}a_l u_m$: $b_k = \epsilon_{klm}a_l u_m/|\epsilon_{hij}a_i u_j|$, by expanding the norm we have: $(\epsilon_{hij}a_i u_j)^2 = 2a^2K - P^2$. We therefore write: $\epsilon_{klm}a_l u_m = b_k\sqrt{2a^2K - P^2} = b_k\sqrt{2K}\sqrt{a^2 - a_T^2} = b_k\sqrt{2K}\sqrt{a_N^2}$.

From (36) the term $D_{ij}D_{ij}$ is computed as [2]

$$D_{ij}D_{ij} = \frac{\gamma^2}{4}\Sigma^2\left(2a^2 + a_T^2\right) \tag{38}$$

We then have

$$a_i M_i = a^2\left(\frac{\alpha}{2\langle K\rangle}P + \frac{\gamma}{2}\Pi - \frac{\gamma}{4}\Sigma^2\right) - a_T^2\frac{\gamma^2}{8}\Sigma^2 \tag{39}$$

To go further we must now specify the terms Π and Σ used for the stochastic process for ε. Various models for the dissipation have been proposed. Pope and Chen [71] proposed a simple model based on the exponential of an Orstein-Uhlenbeck process (see appendix B 2). We rely here on the model proposed by Chevillard [20, 65]. This non-Markovian log-normal model presents a logarithmic decrease in the correlation of ε consistent with the idea of a turbulent cascade and a multiplicative process (see appendix B 1), unlike the Pope model which gives an exponential decrease. As presented in appendix B 2 the drift and diffusion terms are written respectively as:

$$\Pi = \frac{1}{\tau_\varepsilon}\Big(-\ln\frac{\varepsilon}{\langle\varepsilon\rangle} + \frac{\sigma^2}{2\Lambda^2}\big(\frac{\tau_\varepsilon}{\tau_c} - \Lambda^2\big) + \frac{\sigma}{\Lambda}\hat{\Gamma}\tau_\varepsilon\Big) \tag{40}$$

and

$$\Sigma = \sqrt{\frac{\sigma^2}{\Lambda^2\tau_c}} \tag{41}$$

with σ^2 the diffusion coefficient, τ_ε the correlation time of ε, τ_c the regularization time scale of the process, taken equal to the Kolmogorov dissipative time τ_η, and $\hat{\Gamma}$ represents the convolution of the Wiener increments with a temporal kernel and Λ^2 is a normalization factor. The expression for Γ proposed by [20, 65], and recalled in the appendix B 2, applies to a scalar noise as seen in (23) whereas the acceleration model is based on a vectorial noise. We therefore introduced $\hat{\Gamma}$ that applied to the vectorial Wiener increments. For that we modify the definition of Γ by projecting $d\boldsymbol{W}$ before convolving it:

$$\hat{\Gamma} = -\frac{1}{2}\int_{-\infty}^{t}\frac{1}{(t-s+\tau_c)^{3/2}}\mathcal{P}_j dW_j(s) \tag{42}$$

By proceeding in a similar way to the technic proposed by [65], the projection operator is obtained by identification between the diffusion terms of (24) and (28):

$$\mathcal{P}_j = \frac{2a_i D_{ij}}{\gamma a^2\Sigma} = \frac{\sqrt{a_T^2} - a_T}{a^2}a_j + e_j \tag{43}$$

where we have used the relation recall in footnote 1 and e_j is the unit vector tangent to the trajectory $e_i = u_i/\sqrt{2K}$. It is interesting to remark that the rotational part of the diffusion tensor induces an asymmetry of the projector between positive and negative power exchange since $P = \sqrt{2K}a_T$.

Substituting Π and Σ in (39) by (40) and (41) we have

$$a_i M_i = a^2\left(\frac{\alpha}{2\langle K\rangle}P - \frac{\gamma}{2\tau_\varepsilon}\big(\ln\frac{\varepsilon}{\langle\varepsilon\rangle} + \frac{1}{2}\sigma^2 - \frac{\sigma}{\Lambda}\hat{\Gamma}\tau_\varepsilon\big)\right) - a_T^2\frac{\gamma^2}{8}\frac{\sigma^2}{\Lambda^2\tau_c} \tag{44}$$

According to (21) we can write:

$$\ln\left(\frac{\varepsilon}{\langle\varepsilon\rangle}\right) = \frac{1}{\gamma}\left(\ln\frac{a^2}{a_\eta^2} - \ln C - \alpha\frac{K}{\langle K\rangle}\right) \tag{45}$$

---

[2] $D_{ij}D_{ij} = \frac{\gamma^2}{4}\left(a_T^2\underbrace{\delta_{ij}\delta_{ij}}_{3} + a_N^2\underbrace{\epsilon_{ijk}b_k\epsilon_{ijl}b_l}_{2\delta_{kl}b_kb_l}\right)$, and $\delta_{kl}b_kb_l = 1$ since $\boldsymbol{b}$ is a unit vector and with $a^2 = a_T^2 + a_N^2$ we obtain the results.

giving, once substituted into (44):

$$a_i M_i = a^2 \left[\frac{\alpha}{2\langle K\rangle}\left(P+\frac{K}{\tau_\varepsilon}\right) - \frac{1}{2\tau_\varepsilon}\left(\ln\left(\frac{a^2}{a_\eta^2}\right) \underbrace{-\ln C + \frac{\gamma}{2}\sigma^2 - \gamma\frac{\sigma}{\Lambda}\hat{\Gamma}\tau_\varepsilon}_{-\hat{\Gamma}_*} \right) \right] - \frac{a_T^2}{\tau_c}\underbrace{\frac{\gamma^2}{8}\frac{\sigma^2}{\Lambda^2}}_{\sigma_*^2} \tag{46}$$

In order to simplify the notations, we have introduced $\hat{\Gamma}_* = \gamma\frac{\sigma}{\Lambda}\hat{\Gamma}\tau_\varepsilon + \ln C - \frac{\gamma}{2}\sigma^2$ and $\sigma_*^2 = \frac{\gamma^2}{8}\frac{\sigma^2}{\Lambda^2}$ in (46)

We can notice that the term $P + \frac{K}{\tau_\varepsilon} = \frac{dK}{dt} + \frac{K}{\tau_\varepsilon}$ acts as a penalty term leading the correlation of the kinetic energy to decay exponentially.

We then propose for M_i an expression compatible with (46). Proceeding by identification, we have the following relation:

$$\begin{aligned} M_i = & \frac{\alpha}{2\langle K\rangle}\left(\lambda a_i P + (1-\lambda)a^2 u_i + a_i\frac{K}{\tau_\varepsilon}\right) \\ & -a_i\left(\ln\left(\frac{a^2}{a_\eta^2}\right) - \hat{\Gamma}_*\right)\frac{1}{2\tau_\varepsilon} \\ & -\frac{\sigma_*^2}{\tau_c}\frac{a_T^2}{a^2}a_i + B_i \end{aligned} \tag{47}$$

Where we have introduced the vector B_i, such that $B_i a_i = 0$, and the factor λ accounting for the indeterminacy inherent in the "inverse projection". By assuming again that there are only two vectors at our disposal, we can take $B_i = \frac{\alpha}{2\langle K\rangle}\lambda'\left(P a_i - a^2 u_i\right)$ by introducing the factor λ'. Note that from the point of view of the projection, the factors λ and λ' are arbitrary in the sense that the scalar product of a_i and (47) gives (46) whatever their value. We can nevertheless notice that the terms involving λ and λ' can be combined. This shows that the arbitrary choice in the inverse projection or the addition of an orthogonal vector are equivalent, and we get by noting $c_u = \lambda + \lambda'$:

$$\begin{aligned} M_i = & \frac{\alpha}{2\langle K\rangle}\left(a_i\big(c_u P + \frac{K}{\tau_\varepsilon}\big) - (c_u - 1)a^2 u_i\right) \\ & -a_i\left(\ln\left(\frac{a^2}{a_\eta^2}\right) - \hat{\Gamma}_*\right)\frac{1}{2\tau_\varepsilon} \\ & -\frac{\sigma_*^2}{\tau_c}\frac{a_T^2}{a^2}a_i \end{aligned} \tag{48}$$

We can notice that the terms of the first line correspond to the coupling with the velocity, those of the second take account of the log-normal character of the dissipation and the last term is due to the rotational part of the diffusion tensor. The diffusion term (36) becomes, with the expression (41):

$$D_{ij} = \sqrt{\frac{2\sigma_*^2}{\tau_c}}\left[\sqrt{a_T^2}\delta_{ij} + \sqrt{a_N^2}\epsilon_{ijk}b_k\right] \tag{49}$$

We have thus specified our stochastic model for the dynamics of a fluid particle. It is given by (25), (26), (48) and (49).

B. Parameters and numerical approach

From a dimensional point of view, to determine the physical parameters of the stochastic model, one must specify time and velocity scales as well as a Reynolds number. This amounts for example to imposing the average kinetic energy $\langle K\rangle$, the average dissipation rate $\langle\varepsilon\rangle$ and the viscosity ν. Thus, from these physical parameters, we calculate $a_\eta^2 = \langle\varepsilon\rangle^{3/2}\nu^{-1/2}$, $\tau_\eta = \langle\varepsilon\rangle^{-1/2}\nu^{1/2}$. We can also get the Reynolds number based on the Taylor scale $Re_\lambda = u'\lambda/\nu = 2\sqrt{15}/3\,\langle K\rangle/\sqrt{\langle\varepsilon\rangle\nu}$ with $u' = \sqrt{2\langle K\rangle/3}$ and $\lambda^2 = 15\nu u'^2/\langle\varepsilon\rangle$. We then deduce the Lagrangian integral timescale τ_L as $\tau_L = 0.08 Re_\lambda\tau_\eta$ from the DNS results reported by [34, 81].

The parameter σ^2 is estimated using the relation given by [94]: $\sigma^2 \approx 3/8\ln Re_\lambda/R_c$ with $R_c \approx 10$ compatible with the prediction of Kolmogorov and Obhoukov [46, 64]. We set as well $\alpha = 1/3$ and $\gamma = 3/2 + \beta$ with $\beta = -1.33/\ln Re_\lambda$

in accordance with the results of the DNS presented above. The prefactor C is computed as $C = A\,B$ where $A = \left(1 - \frac{2}{3}\alpha\right)^{3/2} \approx 0.686$, $B = 5.8 - 20/\ln Re_\lambda$ as determined by DNS.

For simplicity we have used $\tau_c = \tau_\eta$ and $\tau_\varepsilon = \tau_L$. From τ_ε and τ_η we calculate the value of Λ as explained in B 2. Finally, for the parameter c_u, which is the only free parameter of the model, we have determined numerically that with $c_u = 5.22$ the ratio $K/\langle K\rangle$ is 1 on average for all values of the Reynolds number.

The sample paths of this model were obtained by numerical integration of the stochastic differential equation. Numerical integration is made with an explicit Euler scheme by taking a time-step $dt = \tau_{\eta,min}/100$ with $\tau_{\eta,min} = \sqrt{\nu/\varepsilon_{max}}$ an estimation of the minimum dissipative time scale likely to happen during the simulation. This is estimated from the log-normal distribution of the dissipation: $\tau_{\eta,min} = \tau_\eta \exp(-5.8\sigma/2 + \sigma^2/4)$ by considering that the probability that a random number following the normal distribution reaches a value of 5.8 standard deviation is sufficiently low (see (B11)).

For the calculation of the convolution term $\hat{\Gamma}$ appearing in (48) we propose in appendix B 3 an efficient algorithm.

C. Results

We show in Fig. 7 a realization of this process for $Re_\lambda = 1100$. We see the temporal evolution of the components of acceleration and velocity. There is a very intermittent acceleration with an alternation of periods in which the acceleration of the fluid particle is almost zero with areas of very high activity. This results for the fluid-particle trajectories, obtained by integration of the velocity $x_i = \int u_i(t)dt$, in long quasi-ballistic periods with typical length of the order of the integral scale ($L \approx \langle K\rangle^{3/2}/\langle\varepsilon\rangle$) and short term disruptions during which the trajectory rolls up on itself.

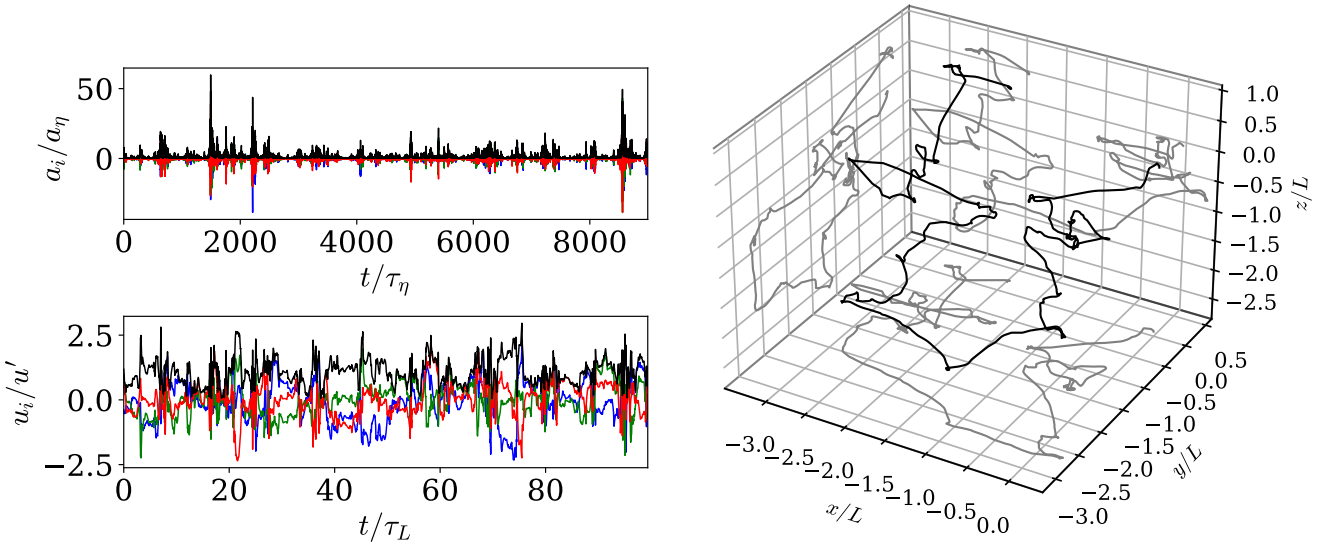

FIG. 7. One realization of the stochastic process for $Re_\lambda = 1100$. Top left: evolution of the acceleration with time, a_x: red, a_y: green, a_z: blue, $|a|$: black. Bottom left: evolution of the velocity with time, u_x: red, u_y: green, u_z: blue, $|u|$: black. Right: 3D trajectory of a fluid particle obtained by time integration of the velocity.

We have simulated the stochastic model for 15 Reynolds numbers between $Re_\lambda = 70$ and 9000. For each case we have computed 26,000 realizations. The simulations are carried out over a period of $120\tau_L$, over which we exclude a transitional regime of $20\tau_L$ for the calculation of the statistics. In all cases, the initial value of the components of acceleration and velocity are sampled from the normal distribution having a standard deviation of $10^{-9}a_\eta$ for the acceleration and $10^{-9}\sqrt{2\langle K\rangle/3}$ for the velocity. We can indeed notice from (48) and (49) that if the acceleration is exactly zero, then the stochastic model predicts that the acceleration would remain so. However, it should be noted that this event has a zero probability, and that for arbitrarily small, but non-zero, accelerations, the model presents evolution towards a non-trivial stationary state. This is illustrated in Fig. 8 which presents the temporal evolution of the variance of the velocity and of the acceleration for $Re_\lambda = 1100$ calculated from all the realizations.

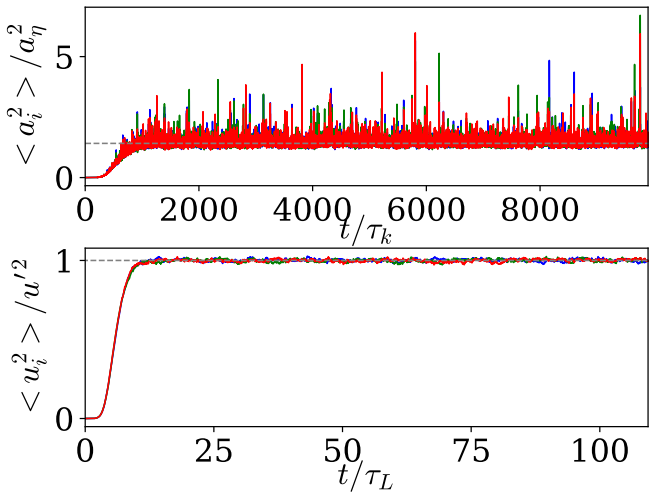

FIG. 8. Evolution of the acceleration and velocity variance with time for $Re_\lambda = 1100$ starting from an initial condition for the acceleration and velocity with very small magnitude. Comparison in dashed gray line with the expected values: (14) for the acceleration and the prescribe value of $u' = \sqrt{2\langle K \rangle/3}$ for the velocity.

Figure 9 shows the evolution with the Reynolds number of the variance of the acceleration and of the mean kinetic energy in the stationary state. We see in this figure that the average kinetic energy is effectively equal, within the statistical convergence, to the value prescribed to the model. Regarding the variance of the acceleration, we expect, by construction of the stochastic model, that the predicted value follows the log-normal relation (14). We observe in Fig. 9, that it is indeed the case, with only very slight deviation for the largest Reynolds numbers which we attributed to numerical errors.

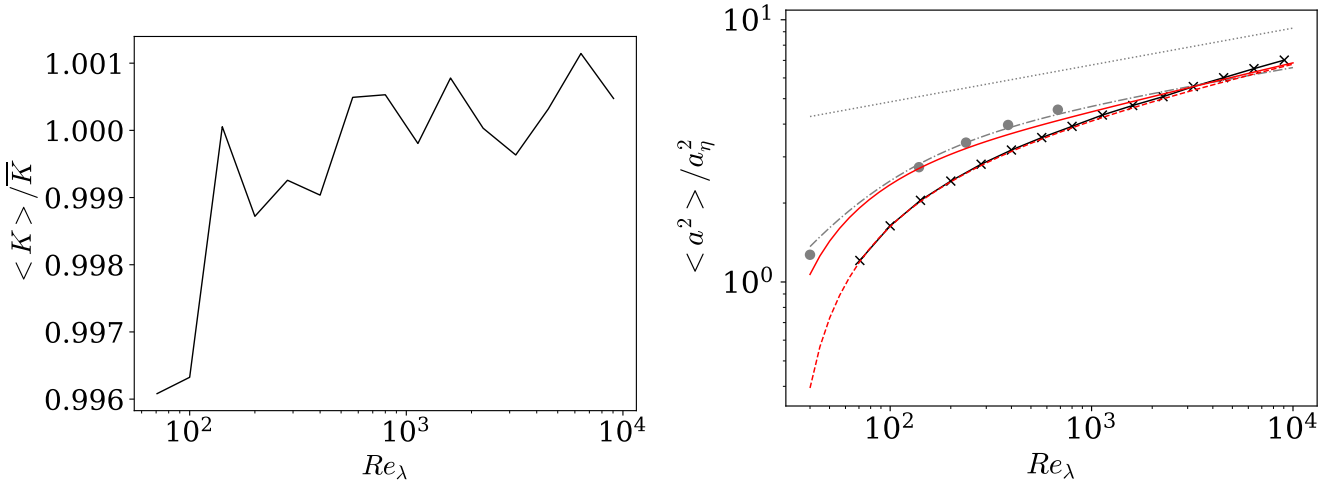

FIG. 9. Evolution with the Reynolds number, in the stationary regime, of the kinetic energy normalized by the prescribed kinetic energy $\overline{K}$ (left) and of the acceleration variance normalized by the Kolmogorov acceleration (right). Data from the Stochastic model (black line with crosses) and comparison with the DNS data from [94] (gray dots), with the relation $1.9Re_\lambda^{0.135}(1 + 85Re_\lambda^{-1.35})$ from [84] (gray dash dot line), with the numerical integration of $\langle a^2 \rangle = \int \langle a^2|\varepsilon\rangle P(\varepsilon) d\varepsilon$ with $\langle a^2|\varepsilon\rangle$ given by (12) and $P(\varepsilon)$ log-normal (continuous red line), with the relation (14) (red dashed line) and with the asymptotic power law (15) (gray dotted line).

Figure 10 compares the autocorrelation for the components of the acceleration and for its norm calculated from the stochastic model for $Re_\lambda = 400$ with the calculations from the DNS of Toschi [8, 50]. It can be seen that the characteristic times of these two quantities are very different and that it is in good agreement with the DNS. It should be mentioned that the scale separation between the components and the norm results from the rotational part of the diffusion tensor. It can indeed be tested that by choosing $c_R = 0$ in equation (35) (corresponding then to a diagonal

diffusion tensor) we do not find this scales separation.

Figure 10 also presents the evolution of the autocorrelation coefficient of the velocity components and the power. It can also be seen here also that the agreement with the DNS is good. In Fig. 10, we also show the evolution of the correlation lengths for these four quantities with the Reynolds number on the range $Re_\lambda = 70 - 9000$ as predicted by the stochastic model. It is seen that when the time shift is normalized by the Kolmogorov time the correlation coefficient of the power and of the acceleration remains nearly unchanged, while the characteristic time scale of the velocity is as expected τ_L. This confirms that the characteristic correlation times for velocity and acceleration components are decoupled. We point out that this decoupling seems directly related to the use of the non-Markovian model for the dissipation used in the derivation of the stochastic model. Indeed by using instead the model proposed by [71] such a decoupling is not observed (but this is not shown to avoid lengthening this document). It should also be noted that the non-Markovian model of [20] proposes a logarithmic evolution of the autocorrelation of the dissipation in agreement with the underlying model of the turbulent energy cascade as discussed in appendix B. This logarithmic evolution is also found for the correlation of the acceleration norm which exhibits a lower slope as the Reynolds number increases, reflecting the absence of characteristic time for its evolution.

The characteristic correlation time for the velocity, the acceleration norm, the components of acceleration and the power are $\tau_u = \int \rho_{u_i}(\tau)d\tau$, $\tau_{|a|} = \int \rho_{|a|}(\tau)d\tau$, $\rho_{a_i} = \int |\rho_{a_i}|(\tau)d\tau$ and $\rho_{a_i} = \int |\rho_P|(\tau)d\tau$. It can be seen that the scale for the norm of the acceleration and for the velocity normalized by the integral scale τ_L remain quasi-constant with the Reynolds number and that the ratio between the correlation scale for the velocity and τ_L is of order 1, while the correlation scales for a component of acceleration and for the power normalized by τ_L vary as $1/Re_\lambda$ as expected.

We show in Fig. 11 the velocity spectrum for Reynolds numbers between $Re_\lambda = 400$ and 9000, which we compare with the DNS of [8] for $Re_\lambda = 400$. We see a very good agreement between the DNS and the stochastic model. For higher Reynolds numbers, we clearly see that a power law behavior develops at intermediate scales. We see that the slope of the power law deviates from the Hinze spectra [87] predicted by dimensional arguments similar to those presented by Kolmogorov, with spectra less stiff than ω^{-2}. This shows that the proposed stochastic model leads to an anomalous scaling reflecting the persistent influence of the Reynolds number on the inertial scales. We further notice that the slope which develops at the intermediate scales are close to $-2 + 0.14$, where 0.14 is the exponent of the asymptotic power law of the acceleration variance with the Reynolds number as determined in (15) (see also Fig. 9). We see here a confirmation of the relation between the acceleration scaling and the anomalous scaling of the velocity spectra proposed by [28].

We present in Fig. 12 the PDF of the velocity, and of the acceleration for $Re_\lambda = 400 \sim 9000$ as well as the comparison with the DNS of [8]. First, we find that the velocity distribution is very close to the Gaussian distribution for all Reynolds numbers, while the acceleration presents a much more stretched distribution. For $Re_\lambda = 400$ the acceleration PDF is in very good agreement with the DNS and for increasing the Reynolds number, the model predicts an increase of the stretching of the tails. We also show in this figure the PDF of the velocity increments for different time shifts $\delta_\tau u_i = u_i(t+\tau) - u_i(t)$. We observe that the distribution gradually returns to the Gaussian distribution as the time shift increases. This is confirmed by the presentation of the flatness of the velocity increments which reflects the strongly non-Gaussian behavior on small scales and gradually decreases to 3 for the larger scales. We also show in the inset a quasi-linear increase of the flatness of the acceleration with the Reynolds number. This relaxation towards the Gaussian is controlled by the term $P + K/\tau_\varepsilon = dK/dt + K/\tau_\varepsilon$ appearing in the drift term of the stochastic model (47).

Finally, in Fig. 13 we show the second and third moments of the power $P = a_i u_i$. It is observed that the increases of both moments with the Reynolds number are in close agreement with the power law supported by the DNS results of [91]. Clearly, the third order moment is negative, meaning that the time irreversibility of the dynamics of a fluid particle in a turbulent flow is correctly reproduced by the proposed stochastic model. The skewness of the power, $S = \langle P^3 \rangle / \langle P^2 \rangle^{3/2}$, seems to converge to -0.5 as the Reynolds number increases as reported in [91].

IV. DISCUSSION AND FINAL REMARKS

In this paper, we have analyzed the behavior of the acceleration statistics conditioned on both local dissipation rate and local kinetic energy, which to our knowledge have not been considered before. We have reported that the doubly conditional variance is proportional to the acceleration variance conditional on the dissipation rate solely, with the proportional factor depending exponentially on the kinetic energy: $\langle a^2|\varepsilon, K\rangle = A \exp(\alpha K/\langle K\rangle)\, \langle a^2|\varepsilon\rangle$. For large enough Reynolds number we show that $A = (1 - 2\alpha/3)^{3/2}$ and we proposed that the α coefficient is independent of the Reynolds number and its value $\alpha = 1/3$ was obtained from the DNS. Such an assumption would require further DNS studies to be validated. As well, it would be interesting to assess the behavior of the doubly conditional acceleration variance for 2D turbulence or in 3D turbulence subjected to mean shears or rotation.

Subsequently, we have proposed to account for the Reynolds number dependence on the acceleration variance

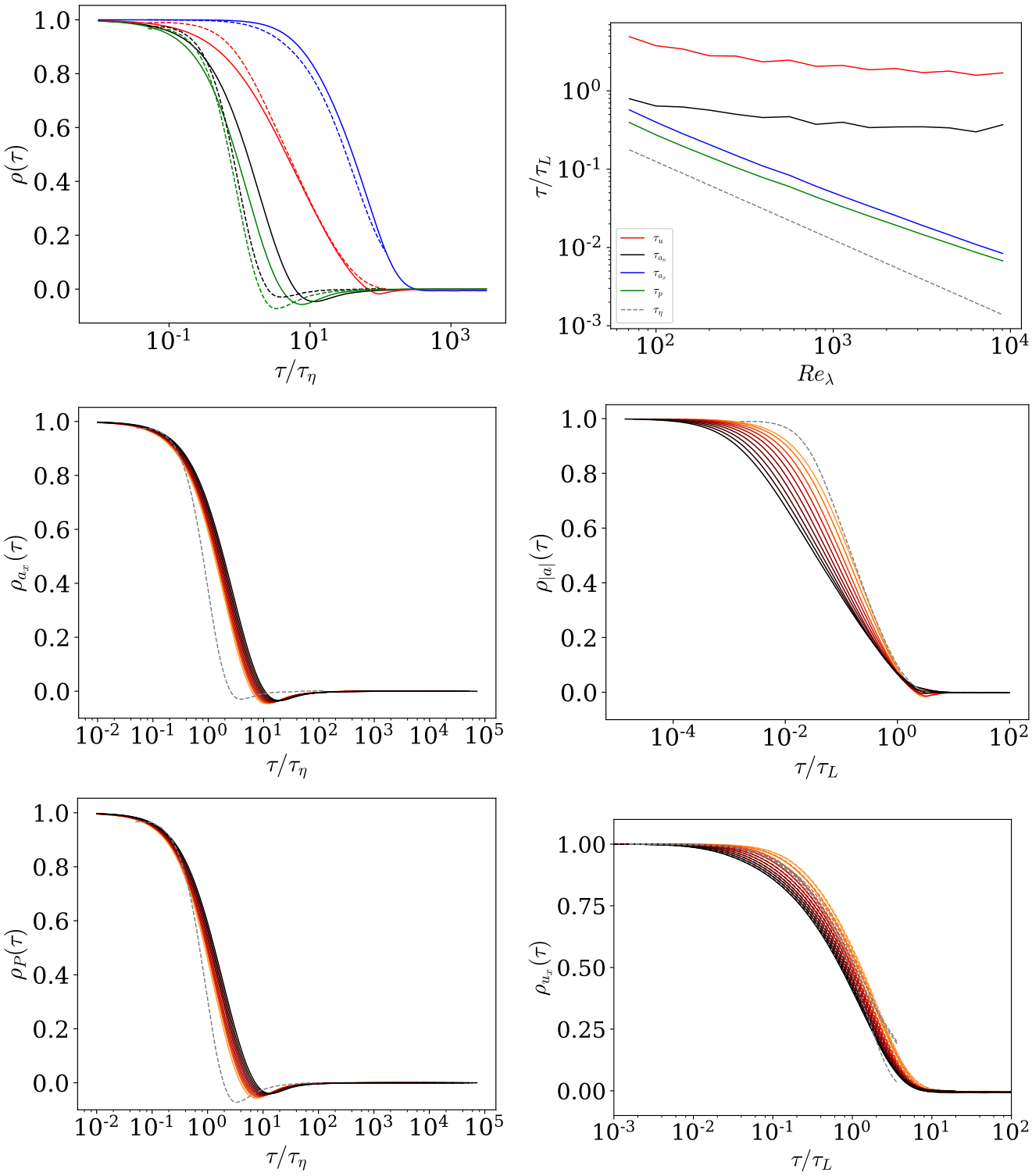

FIG. 10. (a) Evolution of the autocorrelation of a_i (black), $(a^2)^{1/2}$ (red), u_i (blue) and $P = a_i u_i$ (green) from the stochastic model for $Re_\lambda = 400$ and comparison with the DNS data from [8] in dashed line. (b) Evolution of the integral time scale of a_i (black), $(a^2)^{1/2}$ (red), u_i (blue) and $P = a_i u_i$ normalized by τ_L with the Reynolds number. (c,d,e,f) Evolution of the autocorrelation of a_i, $(a^2)^{1/2}$, $P = a_i u_i$ and u_i respectively, for $Re_\lambda = 400$, 567, 800, 1130, 1600, 2263, 3200, 4526, 6400 and 9051 from orange to black and comparison with the DNS data from [8] in dashed line.

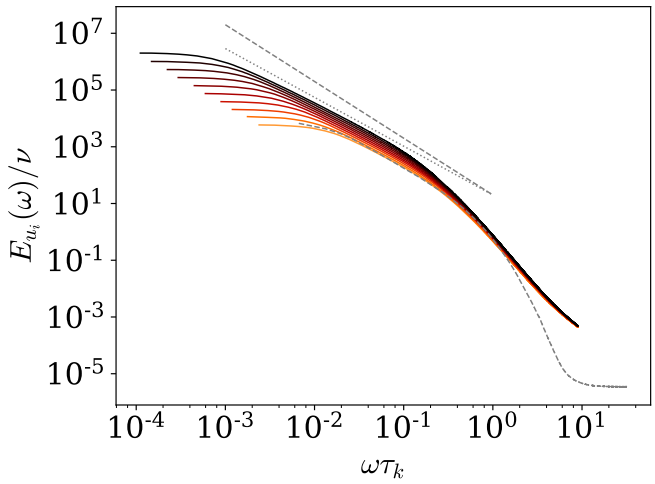

FIG. 11. Velocity spectra from the stochastic model for $Re_\lambda = 400$ to $Re_\lambda = 9000$ from orange to black and comparison with the DNS data from [8] at $Re_\lambda = 400$.

conditional on the dissipation rate within Barenblatt's incomplete similarity framework [6] leading to: $\langle a^2|\varepsilon\rangle = a_\eta^2 B(\varepsilon/\langle\varepsilon\rangle)^{3/2+\beta}$ for $\varepsilon \gg \langle\varepsilon\rangle$ with B and β depending logarithmically on the Reynolds number as the signature of the intermittency and the persistence of viscous effects. As they are slowly evolving function of the Reynolds number, it would require studies over a large range of Reynolds numbers to confirm this proposition and evaluate more precisely the coefficients entering the definition of B and β. On the other hand, as discussed by Barenblatt [6, 32] these coefficients might be determined theoretically from a renormalization group approach. Further, we advance an expression for the conditional acceleration variance valid for the whole range of fluctuations of ε by accounting for the dominance of the large scale sweeping effects in low dissipative regions (see equation (12)). From this finding we determine the evolution of the unconditional acceleration variance with the Reynolds number and show that it is in good agreement with DNS, which gives another empirical validation of the incomplete similarities assumption used to obtain these results.

Finally, for large Reynolds numbers, we propose to express the doubly conditional variance as $\langle a^2|\varepsilon, K\rangle = C\exp(\alpha K/\langle K\rangle + \gamma \ln \varepsilon\langle\varepsilon\rangle)$, $\gamma = 3/2 + \beta$, which is interpreted as a multiplicative cascade for the acceleration that includes the effect of sweeping by all eddies of the turbulence spectrum.

Based on these results we propose a 3D stochastic model for the dynamics of a fluid particle that reproduce the essential features of the Lagrangian dynamics observed from DNS and experiments. To obtain such model, (i) we have assumed, inline with the Kolmogorov universality hypothesis, that the dynamics can be described as a set of stochastic differential equation $da_i = M_i dt + D_{ij} dW_j$; $du_i = a_i dt$, with M_i and a_i depending on the velocity and acceleration along with Reynolds number dependent parameters. (ii) We used the doubly conditional acceleration variance obtained in this paper, to model the instantaneous dynamic relation between acceleration (or force), kinematic energy, and energy dissipation. This amounts to consider that the remains degree of freedom can be discarded in procedure similar to an adiabatic elimination [30] as discussed by [17]. (iii) We introduce a non-diagonal diffusion tensor as well as the maximum winding hypothesis to ensure its physical realizability. (iv) We consider that the dissipation rate along the trajectory is given by the non-Markovian log-normal process proposed recently by [20], giving logarithmic correlation consistently with turbulent cascade picture. With this 4 hypothesis, we obtain the model given by equations (25), (26), (48) and (49) which reads:

$$da_i = \left[\frac{\alpha}{2\langle K\rangle}\left(a_i\left(c_u P + \frac{K}{\tau_\varepsilon}\right) - (c_u - 1)a^2 u_i\right) - a_i\left(\ln\left(\frac{a^2}{a_\eta^2}\right) + \hat{\Gamma}_*\right)\frac{1}{2\tau_\varepsilon} - \frac{\sigma_*^2}{\tau_c}\frac{a_T^2}{a^2}a_i\right]dt$$
$$+\sqrt{\frac{\sigma_*^2}{\tau_c}}\left[\sqrt{a_T^2}\delta_{ij} + \sqrt{a_N^2}\epsilon_{ijk}b_k\right]dW_j \tag{50}$$

We show that the proposed model predicts Lagrangian dynamics presenting non-gausssianity, long-range correlations, anomalous scaling and time irreversibility. Moreover statistics obtained from the stochastic model are in good agreement with the DNS.

In (50) the term proportional to α involves the coupling between velocity and acceleration and allows obtaining a statistically stationary dynamics with one-time Gaussian distribution for the velocity. Introducing a rotational part in

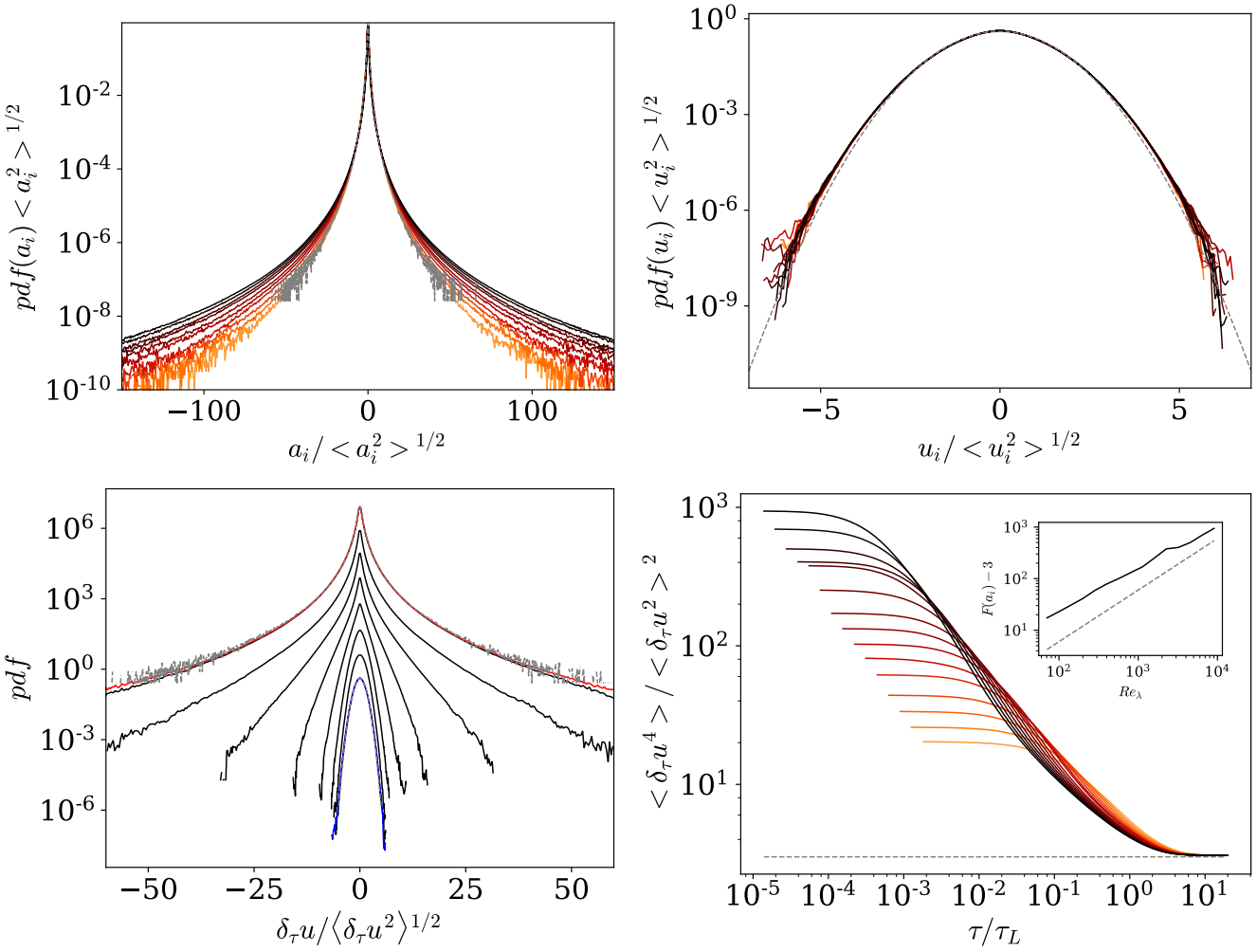

FIG. 12. PDF of a_i(top left) and comparison with the DNS data from [8], and PDF of u_i (top right) and comparison with the normal distribution, for $Re_\lambda = 400$ to 9000 from orange to black. (Bottom left) PDF of the velocity increments for various times shift: $\tau/\tau_\eta = 610$, 200, 70, 22, 7.3, 2.4, 0.8 and 0.25 each time lag is shifted upward by one decade for $Re_\lambda = 400$ comparison with the PDF of the acceleration from the model (red) and from the DNS of [8] (gray) and the PDF velocity (blue). (Bottom right) Evolution of the Flatness of the velocity increments versus the time shift for $Re_\lambda = 70$ to 9000 from orange to black and evolution of the flatness of the acceleration with the Reynolds number and comparison with the linear law in the inset.

the diffusion tensor naturally leads to decomposition of the acceleration vector into its tangential part and its normal components. Since the normal part is associated with the curvature of the trajectory, the rotational part of the diffusion leads to the emergence of a time-scale separation between the correlation of the norm and the components of the acceleration. The term associated with the non-Markovianity of the dissipation along with the rotational part produce an irreversible dynamics, and seen by the skewness of the exchanged power and ensures a scale separation between velocity and acceleration. These three points can be easily checked, by taking $\alpha = 0$ or $c_R = 0$ in (35) or by using for Π the Markovian log-normal dissipation model proposed by [71] rather than the non-Markovian one of of [20].

It is worth noting that from the conditional acceleration statistics obtained from DNS of the Navier-Stokes equation, it is possible to establish, in a fairly natural way, that is to say without using any other hypothesis than the cascade picture, a link between the refined Kolmogorov assumption and the dynamics of fluid particles. It would be interesting to analyze further the stochastic equation to demonstrate the irreversibility of the dynamics, the emergence of anomalous scaling or to study the geometry of the particle trajectory e.g. its curvature and torsion, as well as to further test the conditional statistics between the acceleration and the velocity. We can also mention possible evaluation of the dynamics using the power law model for σ^2 proposed by [17] which can be seen to be close to the logarithmic evolution proposed by [46, 64] on the limited range of Reynolds numbers available to the DNS [94]. Also interesting could be the improvement of the modeling of the high frequency part of the spectrum. Indeed the dissipative part

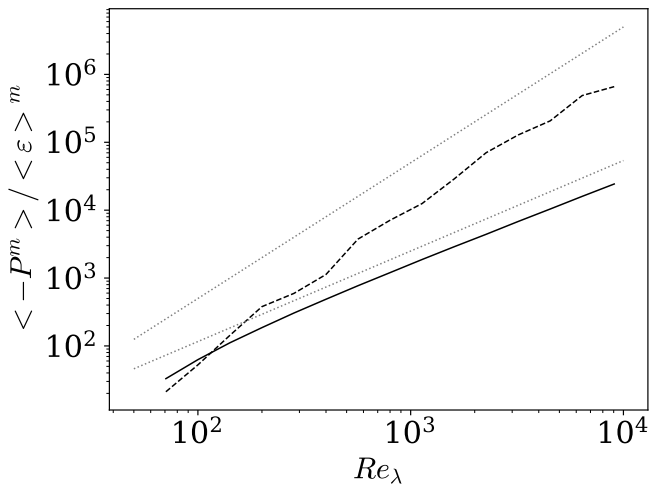

FIG. 13. Evolution of $\langle P^2\rangle/\langle\varepsilon\rangle^2$ and $-\langle P^3\rangle/\langle\varepsilon\rangle^3$ of the power with the Reynolds number, and comparison with the power laws $Re_\lambda^{4/3}$ and Re_λ^2.

of the spectrum is not perfectly reproduced by the model of [20] which intends to model the dissipation rate in the inertial range.

In order to simplify the construction of the model, we have not taken into account the effects of sweeps by the largest structures of the flow, arguing that their effect vanish as the Reynolds number increases (term with a_0^2 in eq. (12)). Based on the relation (12) it is possible to account for the large scale in the stochastic modeling. However, since this term is dependent on the Reynolds number, it is likely that it also depends of the flow configuration. In [33] we have shown how to couple a stochastic model for the particle dynamics with the large eddy simulation (LES) approach predicting the non-universal large-scale behaviors and in [97] we showed that such coupling enables to obtain the saturation of the conditional acceleration in weakly dissipative regions. The propose stochastic model could be further generalized to address shear flows [7] and improve Reynolds-averaged simulations [38, 69]. Finally, let us mention that an interesting extension could be the coupling of the proposed model with stochastic model for the evolution of the velocity gradients as proposed in [31, 39–42, 57, 65], which could be used among other things to improve the calculation of the dynamics of a dispersed phase.

ACKNOWLEDGMENTS

This work has benefited from stimulating discussions with R. Letournel, L. Goudenège, A. Vié, A. Richard and M. Massot. A. Lanottte, E. Calzavarini, F. Toschi, J. Bec, L. Biferale and M. Cencini are thanked for making the DNS dataset "Heavy particles in turbulent flows" (2011) publicly available from the International CFD Database [50]. Our DNS simulations were performed using high-performance computing resources from GENCI-CINES and GENCI-IDRIS (grant A0112B07400) and the CALMIP Centre of the University of Toulouse (grant P0910).

Appendix A: Determination of c_ε

To evaluate the c_ε factor appearing in (1), we use the following relation between the conditional averages [3]:

$$\langle a^2|\varepsilon\rangle = \int dK \langle a^2|\varepsilon, K\rangle P(K|\varepsilon) \tag{A1}$$

Substituting relation (1) in (A1), we find, assuming that c_ε is independent of K

$$\langle a^2|\varepsilon\rangle/a_\eta^2 = c_\varepsilon \int dK \exp(\alpha K/\langle K\rangle) P(K|\varepsilon) \tag{A2}$$

[3] This relation is simply obtained from the relation between the joint PDF and the conditional PDF: $P(a^2,\varepsilon,K) = P(a^2|\varepsilon,K)P(\varepsilon,K) = P(a^2|\varepsilon,K)P(K|\varepsilon)P(\varepsilon)$ and the relation between the joint probability density of a^2,ε,K and a^2,ε: $P(a^2,\varepsilon) = \int dK P(a^2,\varepsilon,K)$.

This clearly demonstrate that if the kinetic energy is statistically independent of the dissipation rate (*i.e.* $P(K|\varepsilon) = P(K)$) the integral in the previous relation takes a constant value and c_ε is proportional to $\langle \boldsymbol{a}^2|\varepsilon\rangle$. However such an assumption is only approximate at moderate Reynolds numbers as shown from our DNS. Indeed, it is seen in Fig. 14(a), that the average of K conditioned on ε has a weak logarithmic dependence on ε. We also present in Fig. 14(b) the probability density of the kinetic energy conditioned on the dissipation rate. In this figure, the PDF is normalized by its mean value $\langle K|\varepsilon\rangle$. It is to note that for large values of the dissipation rate, the conditional PDF takes a self-similar form:

$$P(K/\langle K|\varepsilon\rangle|\varepsilon) = P_G(K/\langle K|\varepsilon\rangle) \tag{A3}$$

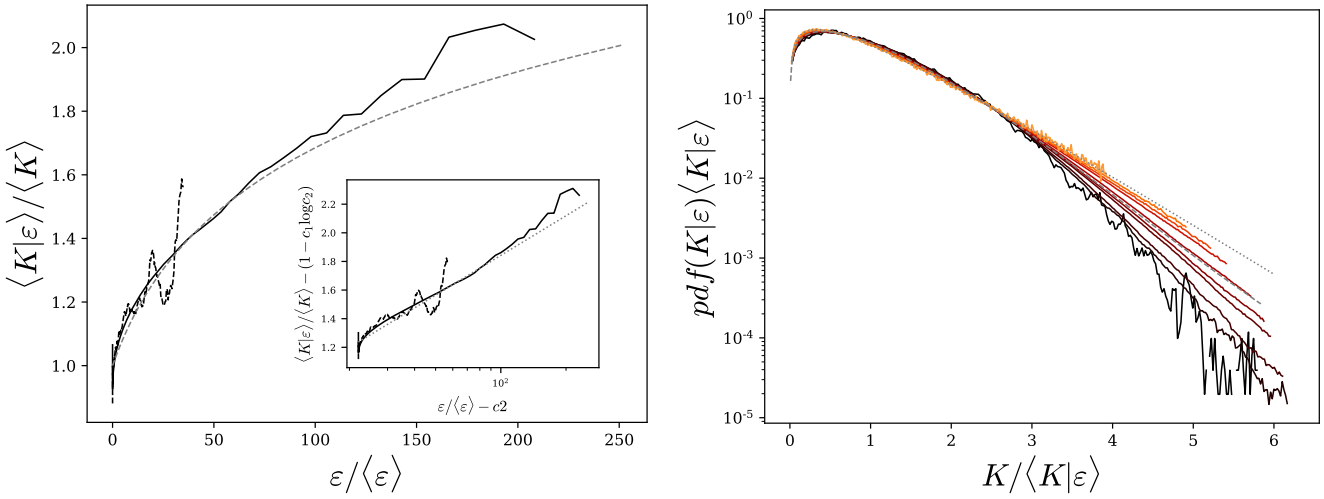

FIG. 14. (a) Average of the kinetic energy conditioned on the local dissipation rate from our DNS in continuous line and from DNS database of [8, 50] in dashed line and comparison with the relation $\langle K|\varepsilon\rangle/\langle K\rangle \approx 1 + c_1 \log\left(c_2^{-1}\varepsilon/\langle\varepsilon\rangle + 1\right)$ with $c_1 = 2/5$ and $c_2 = 22$ in dotted line. Insert : evolution of $\langle K|\varepsilon\rangle - (1 - c_1 \log c_2)$ as a function of $\varepsilon/\langle\varepsilon\rangle + c_2$, and comparison with $\langle K|\varepsilon\rangle/\langle K\rangle - (1 - c_1 \log c_2) = c_1 \log(\varepsilon/\langle\varepsilon\rangle + c_2)$. (b) Probability density function of the Kinetic energy conditioned on the dissipation rate, normalized by its average $\langle K|\varepsilon\rangle$. Comparison with the marginal PDF of the kinetic energy in dashed line and with the PDF (A5) in dotted line.

Thus by combining the previous relations, one can write:

$$\langle a^2|\varepsilon\rangle/a_\eta^2 = c_\varepsilon \int dK^* \exp(\alpha^* K^*) P_G(K^*) \tag{A4}$$

where we have introduced $K^* = K/\langle K|\varepsilon\rangle$ and $\alpha^*(\varepsilon) = \alpha \langle K|\varepsilon\rangle/\langle K\rangle$. In addition, we see in Fig. 14(b) that the self-similar form of the distribution of K^* knowing ε is well approximated by the following distribution obtained from the Maxwell distribution (i.e. assuming that the three components of the velocity are Gaussian and independent):

$$P_G(x) = \frac{3}{\sqrt{\pi}} \sqrt{\frac{3}{2}x} \exp\left(-\frac{3}{2}x\right) \tag{A5}$$

Note that the average of this distribution is indeed unity: $\int x P_G(x) dx = 1$. With this expression for P_G the integral of equation (A4) can be compute as: $\int dK^* \exp(\alpha^* K^*) P_G(K^*) = \left(1 - \frac{2}{3}\alpha^*\right)^{-3/2} = A_\varepsilon^{-1}$. Thus, according to (A2), we have for c_ε:

$$c_\varepsilon = A_\varepsilon \langle a^2|\varepsilon\rangle/a_\eta^2 \tag{A6}$$

The dependence of A_ε with ε explains the deviation of the power law behavior between $\langle a^2|\varepsilon, K\rangle$ and $\langle a^2|\varepsilon\rangle$ observed in Fig. 2b for $\varepsilon \gg \langle\varepsilon\rangle$.

It is to note that the integral A_ε converges only if $\alpha^* < 3/2$. This observation implies that the dependence of $\langle K|\varepsilon\rangle/\langle K\rangle$ on ε should decrease as the Reynolds number increases to allow α^* to remains lower than 3/2 even for

the most intense fluctuations of $\varepsilon/\langle\varepsilon\rangle$, and thus ensuring the convergence of the integral. Therefore, the larger the Reynolds number, the weaker the dependence of $\langle K|\varepsilon\rangle/\langle K\rangle$ on ε, confirming that within the limit of large Reynolds numbers the local values of the kinetic energy and of the dissipation become statistically independent in line with scale separation of the turbulent cascade. Accordingly, we simply propose to write:

$$c_\varepsilon \approx A\,\langle a^2|\varepsilon\rangle/a_\eta^2 \tag{A7}$$

where $A = \left(1-\frac{2}{3}\alpha\right)^{3/2}$, which is equal to $A = 7\sqrt{7}/27 \approx 0.686$, for $\alpha = 1/3$, neglecting the small logarithmic dependence in $\varepsilon/\langle\varepsilon\rangle$.

Appendix B: Modeling of the dissipation rate

1. Dissipation as multiplicative cascade process

The image of the energy cascade is naturally associated with multiplicative processes [45, 59, 92]. Such model proposes to express the locally space-averaged dissipation over a volume of size $\ell = L\lambda^n$, with L the large scale of the flow and $\lambda < 1$, as:

$$\varepsilon_n = \varepsilon_0 \frac{\varepsilon_1}{\varepsilon_0} \cdots \frac{\varepsilon_n}{\varepsilon_{n-1}} = \varepsilon_0 \prod_{i=1}^{n} \xi_i \tag{B1}$$

Assuming that $\xi_i = \varepsilon_i/\varepsilon_{i-1}$ are independent randoms numbers with identical distribution across scales we write:

$$\log \frac{\varepsilon_n}{\varepsilon_0} = \sum_{i=1}^{n} \log \xi_i \tag{B2}$$

Therefore according to the central limit theorem the term on the right must present a normal distribution with parameters $\mu = n\mu_\xi$ and $\sigma^2 = n\sigma_\xi^2$. The parameters μ_ξ et σ_ξ^2 appear as fundamental unknowns, but can nevertheless be related by the relation $\mu_\xi = -\sigma_\xi^2/2$ obtained from the moments of a log-normal variable in order to guarantee that the average energy flux is conserved throughout the cascade. Setting $\ell = \eta$ (i.e. $n = \ln(\eta/L)/\ln\lambda \sim \ln Re_\lambda$) we obtain a model for the local dissipation rate. The log-normal distribution for ε has been confirmed for example by DNS of [94]. Moreover for the variance of logarithm of the local dissipation rate is then $\sigma^2 = \frac{\sigma_\xi}{\ln\lambda}\ln\eta/L = A + B\ln Re_\lambda$ as predicted by Kolmogorov and Oboukhov [46, 64]. Such evolution for σ^2 has been also confirmed from the DNS of [94] showing that $\sigma^2 \approx 3/8\ln Re_\lambda/10$.

Such multiplicative process also imply a logarithmic evolution of the spatial correlation of the dissipation rate as explained by Mandelbrot [55]. We consider the dissipation rate at two points A and B, ε_n^A and ε_n^B, both defined at the same scale n. The points A and B are separated by a distance $L > r > \eta$ from each other and we note $k = \ln(r/L)/\ln\lambda$, then $0 < k < n$. Clearly, the greater the distance between the two points, the larger the scale of their common root in the cascade:

$$\varepsilon_n^A = \varepsilon_0^{AB} \frac{\varepsilon_1^{AB}}{\varepsilon_0^{AB}} \cdots \frac{\varepsilon_k^{AB}}{\varepsilon_{k-1}^{AB}} \frac{\varepsilon_{k+1}^{A}}{\varepsilon_k^{A}} \cdots \frac{\varepsilon_n^{A}}{\varepsilon_{n-1}^{A}} \tag{B3}$$

$$\varepsilon_n^B = \varepsilon_0^{AB} \frac{\varepsilon_1^{AB}}{\varepsilon_0^{AB}} \cdots \frac{\varepsilon_k^{AB}}{\varepsilon_{k-1}^{AB}} \frac{\varepsilon_{k+1}^{B}}{\varepsilon_k^{B}} \cdots \frac{\varepsilon_n^{B}}{\varepsilon_{n-1}^{B}} \tag{B4}$$

In the two previous equations we have distinguished by the exponents A and B the variables which are specific to points A and B and by AB those which are common. This can be expressed as:

$$\ln \frac{\varepsilon_n^A}{\varepsilon_0} = \sum_{i=1}^{k} \ln \xi_i^{AB} + \sum_{i=k+1}^{n} \ln \xi_i^{A} \tag{B5}$$

$$\ln \frac{\varepsilon_n^B}{\varepsilon_0} = \sum_{i=1}^{k} \ln \xi_i^{AB} + \sum_{i=k+1}^{n} \ln \xi_i^{B} \tag{B6}$$

The correlation between $\ln \varepsilon_n^A$ and $\ln \varepsilon_n^B$ is defined as

$$R_{\ln \varepsilon}(r) = \langle (\ln \frac{\varepsilon_n^A}{\varepsilon_0} - \mu)(\ln \frac{\varepsilon_n^B}{\varepsilon_0} - \mu) \rangle = \langle \ln \frac{\varepsilon_n^A}{\varepsilon_*} \ln \frac{\varepsilon_n^B}{\varepsilon_*} \rangle \tag{B7}$$

where we noted $\varepsilon_* = \varepsilon_0 e^{\mu}$. Introducing similarly $\xi_* = e^{\mu_\chi}$ and $\xi' = \xi/\xi_*$ we express the correlation as:

$$\begin{aligned}
R_{\ln \varepsilon} &= \langle \sum_{i=1}^{n} (\ln \xi_i^A - \mu_\xi) \sum_{j=1}^{n} (\ln \xi_i^B - \mu_\xi) \rangle = \langle \sum_{i=1}^{n} \ln {\xi'_i}^A \sum_{j=1}^{n} \ln {\xi'_j}^B \rangle \\
&= \langle \left(\sum_{i=1}^{k} \ln {\xi'_i}^{AB} + \sum_{i=k+1}^{n} \ln {\xi'_i}^A \right) \left(\sum_{j=1}^{k} \ln {\xi'_j}^{AB} + \sum_{j=k+1}^{n} \ln {\xi'_j}^B \right) \rangle \\
&= \sum_{i=1}^{k} \sum_{j=1}^{k} \langle \ln {\xi'_i}^{AB} \ln {\xi'_j}^{AB} \rangle + \sum_{i=1}^{k} \sum_{j=k+1}^{n} \langle \ln {\xi'_i}^{AB} \ln {\xi'_j}^{AB} \rangle \\
&\quad + \sum_{i=k+1}^{n} \sum_{j=1}^{k} \langle \ln {\xi'_i}^{A} \ln {\xi'_j}^{AB} \rangle + \sum_{i=k+1}^{n} \sum_{j=k+1}^{n} \langle \ln {\xi'_i}^{AB} \ln {\xi'_j}^{B} \rangle \\
&= \sum_{i=1}^{k} \sum_{j=1}^{k} \delta_{ij} \sigma_\xi^2 = k \sigma_\xi^2
\end{aligned} \tag{B8}$$

To obtained this results we used the hypothesis that within the same branch, the events at a given scale are independent of those at another scale, $\langle \ln {\xi'_i}^{AB} \ln {\xi'_j}^{AB} \rangle = \delta_{ij} \sigma_\xi^2$, as well as vanishing correlation between branches A and B: $\langle \ln {\xi'_i}^{A} \ln {\xi'_j}^{B} \rangle = 0$. This gives a logarithmic evolution of the correlation coefficient $\rho_{\ln \varepsilon} = R_{\ln \varepsilon}/\sigma^2$, in the range $\eta < r < L$:

$$\rho_{\ln \varepsilon} = \frac{\langle \ln \frac{\varepsilon_n^A}{\varepsilon_*} \ln \frac{\varepsilon_n^B}{\varepsilon_*} \rangle}{\langle \ln^2 \frac{\varepsilon_n}{\varepsilon_*} \rangle} = \frac{k}{n} = \frac{\ln L/r}{\ln L/\eta} = 1 - \frac{\ln r/\eta}{\ln L/\eta} \tag{B9}$$

Although not trivial, this result can be transpose for the temporal correlation along particle path [13, 37, 58, 83]. The logarithmic behavior of the correlation is confirmed by DNS, as it can be seen in [54] where the evolution of the Lagrangian correlation of the logarithm of the dissipation is presented.

2. Stochastic Modeling of the dissipation

It has been proposed to model the dissipation rate as stochastic multiplicative process. Such process can be generically expressed as :

$$d\varepsilon = \varepsilon \Pi dt + \varepsilon \Sigma dW \tag{B10}$$

with dW the increment of the Wiener process ($\langle dW = 0$ and $\langle dW^2 \rangle = dt$) and where Π and Σ are to be determined.

Considering that ε follows a log-normal distribution with parameter σ^2 and $\mu = -\sigma^2/2$, we define the standard normal variable χ (Gaussian random variable with zero mean and unit variance) as:

$$\frac{\varepsilon}{\langle \varepsilon \rangle} = \exp\left(\sigma \chi - \sigma^2/2\right) \tag{B11}$$

A stochastic process for χ has to be given in order to obtain the stochastic process for ε, via the Ito transformation. Pope and Chen [71] proposed to obtain χ from an Orstein-Uhnlebbeck process with a characteristic time τ_ε:

$$d\chi = -\frac{\chi}{\tau_\varepsilon} dt + \sqrt{\frac{2}{\tau_\varepsilon}} dW \tag{B12}$$

According to the Ito formula this gives for Π and Σ :

$$\Pi = -\left(\ln \varepsilon/\langle \varepsilon \rangle - \sigma^2/2\right)/\tau_\varepsilon \tag{B13}$$

$$\Sigma = \sqrt{2\sigma^2/\tau_\varepsilon} \tag{B14}$$

This process gives as expected log-normal distribution for ε (normal distribution for χ) as well as an exponential decrease of the correlation of $\ln \varepsilon$ with a characteristic time τ_ε. This exponential behavior is not consistent with the multiplicative cascade model as discuss above. It rather correspond to a direct energy transfer from large to small scales.

To ensure a logarithmic decorrelation of the dissipation, Chevillard [20] proposed to adapt the Gaussian multiplicative chaos introduced by Mandelbrot [55]. This leads to a multifractal model in which the Wiener process in (B12) is replace by a fractional Gaussian noise:

$$d\chi = -\frac{\chi}{\tau_\varepsilon}dt + \frac{1}{\Lambda}dW^0_{\tau_c} \tag{B15}$$

here, $dW^0_{\tau_c}$ is formally a fractional Gaussian noise with a 0 Hurst exponant, regularized at a time scale τ_c, and Λ is a normalization factor ensuring unit variance for χ. The value of Λ is dependent on the specific regularization of $dW^0_{\tau_c}$. As explained in [20] this process can be reexpressed as

$$d\chi(t) = \left(-\frac{\chi}{\tau_\varepsilon} + \frac{\Gamma}{\Lambda}\right)dt + \frac{1}{\sqrt{\Lambda^2\tau_c}}dW \tag{B16}$$

with dW the increments of a standard Wiener process and Γ corresponds to a convolution of the Wiener increments:

$$\Gamma = -\frac{1}{2}\int_{-\infty}^{t}(t-s+\tau_c)^{-3/2}dW(s) \tag{B17}$$

where $dW(s)$ is the increments of the same realization of the wiener process as in (B16). In (B17), the regularization time τ_c prevent the divergence of the kernel when $s \to t$. The normalization factor Λ is estimated as $\Lambda = \langle X^2 \rangle$ where X obey the stochastic equation (B16) in which Λ has been set to 1.

The stochastic process (B16) give a logarithmic correlation for χ: $\langle \chi(t)\chi(t-s)\rangle \sim \ln \frac{\tau_\varepsilon}{s}$ for $\tau_c \ll s \ll \tau_\varepsilon$, as illustrated in the Fig. 15.

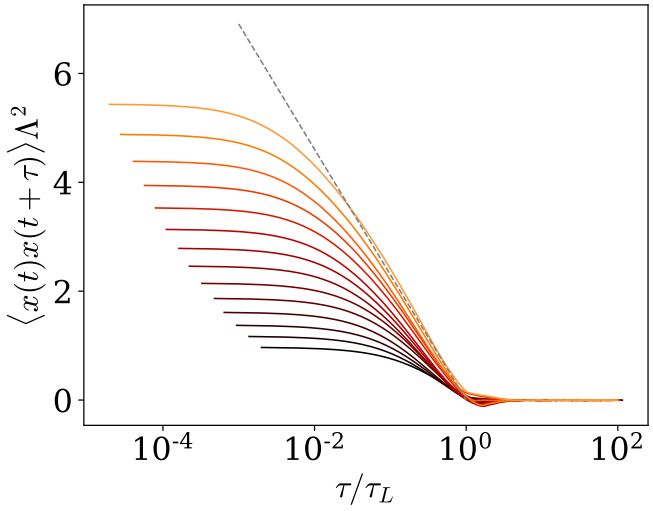

FIG. 15. Correlation de χ for various value of τ_ε/τ_c.

With the Ito transformation, we obtain the process for ε from (B16). this gives for Π and Σ :

$$\Pi = \left(-\ln\frac{\varepsilon}{\langle\varepsilon\rangle} + \frac{\sigma^2}{2\Lambda^2}\left(\frac{\tau_\varepsilon}{\tau_c} - \Lambda^2\right) + \frac{\sigma}{\Lambda}\Gamma\tau_\varepsilon\right)/\tau_\varepsilon \tag{B18}$$

$$\Sigma = \sqrt{\frac{\sigma^2}{\Lambda^2\tau_c}} \tag{B19}$$

3. Efficient calculation of the stochastic convolution Γ

In order to obtain a stationary process the lower bound of the integration is set to $-\infty$. For the numerical computation of this integral, the lower limit have to be truncated. We present in figure 16 one realization of the evolution of the integral $\Gamma(t,\tau) = -\frac{1}{2}\int_{t-\tau}^{t}(t-s+\tau_c)^{-3/2}dW(s)$ when the lower bound varies. We see that for values larger than τ_ε the integral converges to a value (which remains random). In addition, the convergence threshold does not seem to depend on the time step used. So in practice Γ will be calculated with a lower bound set to $t-\tau_\varepsilon$.

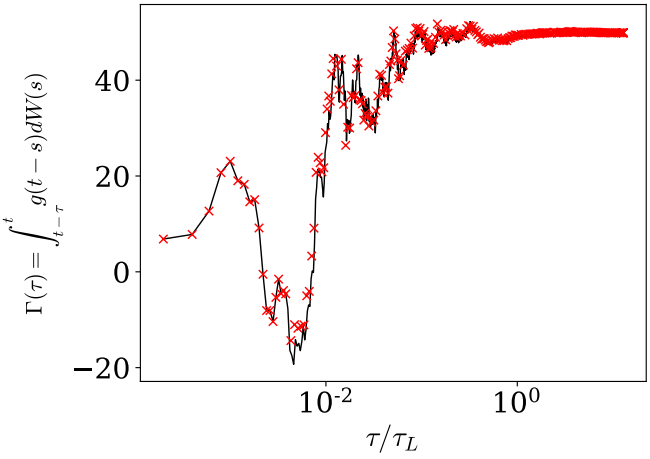

FIG. 16. One realization of the integral (B17) as a function of the lower bound of the integral for $dt = \tau_c/100$. Comparison between the direct calculation of the history integral (B17) (black line) and the optimized calculation with $N_s = 12$ (red crosses).

To obtain these calculations, the integral (B17) giving the value of Γ at time $t_n = n\,dt$ has been discretized as proposed by [20]

$$\Gamma_n = -\frac{1}{2}\sum_{m=0}^{N_{hist}}(s_m+\tau_c)^{-3/2}\,dW_{n-m} \tag{B20}$$

with $s_m = t_n - t_{n-m} = m\,dt$, $N_{hist} = \tau_\varepsilon/dt$ and dW_{n-m} the increment of the Wiener process at time $(n-m)dt$.

This direct calculation requires a lot of memory in order to keep the last N_{hist} instants and requires a very large number of operations, of the order of $N_t \times N_{hist}$ where N_t is the number of time step of the simulation. Thus this direct method is difficult to use in practice when $\tau_\varepsilon/\tau_\eta \sim Re_\lambda$ becomes large.

For this reason [20] proposed to speed up significantly the calculation using the fast Fourier transforms (FFT). The integral at time $n\,dt$ is then computed as $\Gamma_n = -1/2 z_n$ where $z_n = FFT^{-1}(Z_k)$ is given by the inverse Fourrier transform of Z_k. $Z_k = X_k\,Y_K$ is the convolution in spectral space between x_n and y_n ($X_k = FFT(x_n)$ and $Y_k = FFT(y_n)$) where x_n et y_n are the sequences dW_n and $(s_n+\tau_x)^{-3/2}$ padded with zeros such that they have $N > N_{hist} + N_t$ points. This algorithm is indeed much faster. Nevertheless, the memory occupation becomes more important since all the values of the sequence dW_n must be known simultaneously in order to calculate the Fourier transform, which limits the possibility of using this algorithm for large Reynolds numbers.

Such limitation can be overcome by using the approach proposed in [54] based on the inverse Laplace transform of the convolution Kernel. In this approach Γ is estimated as a weighted sum of correlated Orstein-Uhlenbeck processes with characteristic time ranging from τ_c to τ_ε.

Despite its efficiency, this technic, nor the one based on FFT, cannot be used to determine the $\hat{\Gamma}$ that appears in the vectorial stochastic model for the acceleration, or as noted by [65] for velocity gradients. Indeed in such cases it is not the increments of the components of the Wiener process which are convoluted, but a projection of them as shown in (42). The issue is that the projection cannot by computed a priori, because it requires knowing a_i and u_i, as seen in (43).

For this raisons we propose a new algorithm which is fast, using a limited amount of memory and which only requires knowing the dW_n sequentially. This algorithm is derived from the one introduced for non-stochastic integrals in [53]. As we go back in the past, we can afford to remember with less precision the noise entering this integral, since the kernel decreases with the lag. We will thus proceed by progressive "coarse graining" and group together

the oldest dW_n, by introducing an increasingly extended local average. We then decompose the sum of (B20) into sub-sums comprising an increasing number of terms:

$$\begin{aligned}
-2\Gamma_n &= \sum_{m=0}^{N_{hist}} (s_m+\tau_c)^{-3/2}\, dW_{n-m} \\
&= \sum_{m=m_{s1}}^{m_{e1}} (s_m+\tau_c)^{-3/2}\, dW_{n-m} + \ldots + \sum_{m=m_{sN}}^{m_{eN}} (s_m+\tau_c)^{-3/2}\, dW_{n-m} \\
&= \sum_{j=1}^{N} \sum_{m=m_{sj}}^{m_{ej}} (s_m+\tau_c)^{-3/2}\, dW_{n-m} \\
&\approx \sum_{j=1}^{N} (\overline{s}_j+\tau_c)^{-3/2}\, \overline{dW}_j
\end{aligned} \tag{B21}$$

Where we introduced $\overline{s}_j = (m_{ej}+m_{sj})dt/2$ and $\overline{dW}_j = \sum_{m=m_{sj}}^{m_{ej}} dW_{n-m}$ such that $(\overline{s}_j+\tau_c)^{-3/2}\,\overline{dW}_j \approx \sum_{m=m_{sj}}^{m_{ej}} (s_m+\tau_c)^{-3/2}\, dW_{n-m}$. The bounds m_{ej} and m_{sj} are progressively spaced as j increases leading to an increasingly coarse splitting of the integral. This approximation of the integral can be carried out very efficiently by using a non-homogeneous list updating for $\overline{dW}$. The first elements of the list are updated every time step and the older ones less and less regularly, as described in the diagram of Fig. 17). In detail, we update the first N_s elements of the list at each time step, the following N_s every two time steps, and the elements between iN_s and $(i+1)N_s$ are only updated every 2^i iterations. Thus, with $n \times N_s$ elements in the list we can estimate the integral going up to $\sum_{i=0}^{n} N_s\, 2^i dt = 2N_s(2^n-1)dt$ in the past. This gives a considerable saving in computation time and memory with a good accuracy as it is illustrated in Fig. 16. For all the calculation presented in this paper we have used $N_s = 12$.

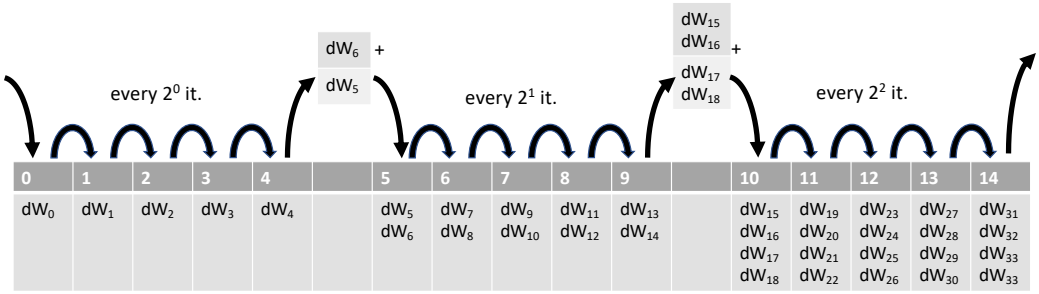

FIG. 17. Diagram illustrating the coarse-graining of the integral (B17) and the non-uniform update of the list.

[1] A. K. Aringazin and M. I. Mazhitov. stochastic models of Lagrangian acceleration of fluid particle in developed turbulence. *International Journal of Modern Physics B*, 18:3095–3168, 2004.

[2] A. Arneodo, R. Benzi, J. Berg, L. Biferale, E. Bodenschatz, A. Busse, E. Calzavarini, B. Castaing, M. Cencini, L. Chevillard, R. T. Fisher, R. Grauer, H. Homann, D. Lamb, A. S. Lanotte, E. Lévêque, B. Luthi, J. Mann, N. Mordant, W.-C. Muller, S. Ott, N. T. Ouellette, J.-F. Pinton, S. B. Pope, S. G. Roux, F. Toschi, H. Xu, and P. K. Yeung. Universal Intermittent Properties of Particle Trajectories in Highly Turbulent Flows. *Physical Review Letter*, 100:250504, 2008.

[3] E. Bacry, J. Delour, and J. F. Muzy. Multifractal random walk. *Physical Review E*, 64(2):026103, 2001.

[4] G. I. Barenblatt. *Scaling*. Cambridge University Press, Cambridge, U.K., 2002.

[5] G. I. Barenblatt and A. J. Chorin. New perspectives in turbulence: scaling laws, asymptotics, and intermittency. *SIAM Rev.*, 40(2):265–291, 1998.

[6] G.I. Barenblatt and A.J. Chorin. A mathematical model for the scaling of turbulence. *Proc. Nat. Acad. Sc. USA*, 101:15023–15026, 2004.

[7] A. Barge and M. A. Gorokhovski. Acceleration of small heavy particles in homogeneous shear flow: direct numerical simulation and stochastic modelling of under-resolved intermittent turbulence. *Journal of Fluid Mechanics*, 892:A28, 2020.

[8] J. Bec, L. Biferale, M. Cencini, A. Lanotte, and F. Toschi. Intermittency in the velocity distribution of heavy particles in turbulence. *Journal of Fluid Mechanics*, 646:527–536, 2010.

[9] C. Beck. Lagrangian acceleration statistics in turbulent flows. *EPL (Europhysics Letters)*, 64(2):151, 2003.

[10] L. Biferale, E. Bodenschatz, M. Cencini, A. S. Lanotte, N. T. Ouellette, F. Toschi, and H. Xu. Lagrangian structure functions in turbulence: A quantitative comparison between experiment and direct numerical simulation. *Physics of Fluids*, 20(6):065103, 2008.

[11] L. Biferale, G. Boffetta, A. Celani, B.J. Devenish, A. Lanotte, and F. Toschi. Multifractal Statistics of Lagrangian Velocity and Acceleration in Turbulence. *Physical Review Letter*, 93:064502, 2004.

[12] L. Biferale and F. Toschi. Joint statistics of acceleration and vorticity in fully developed turbulence. *Journal of Turbulence*, 6(40), 2006.

[13] M. S. Borgas. The Multifractal Lagrangian Nature of Turbulence. *Philosophical Transactions: Physical Sciences and Engineering*, 342(1665):379–411, 1993.

[14] M. S. Borgas and P. K. Yeung. Conditional fluid-particle accelerations in turbulence. *Theoretical and computational fluid dynamics*, 11(2):69–93, 1998.

[15] W. J. T. Bos and R. Zamansky. Power fluctuations in turbulence. *Physical Review Letters*, 122(12):124504, Mar 2019.

[16] B. Castaing. The temperature of turbulent flows. *Journal de Physique II*, 6:105–114, 1996.

[17] B. Castaing, Y. Gagne, and E.J. Hopfinger. Velocity probability density functions of high Reynolds number turbulence. *Physica D: Nonlinear Phenomena*, 46(2):177–200, 1990.

[18] B. Castaing, Y. Gagne, and M. Marchand. Log-similarity for turbulent flows? *Physica D: Nonlinear Phenomena*, 68(3-4):387–400, 1993.

[19] S. Chen and R. H. Kraichnan. Sweeping decorrelation in isotropic turbulence. *Physics of Fluids A: Fluid Dynamics (1989-1993)*, 1(12):2019–2024, 1989.

[20] L. Chevillard. Regularized fractional Ornstein-Uhlenbeck processes and their relevanceto the modeling of fluid turbulence. *Physical Review E*, 96:033111, 2017.

[21] L. Chevillard, S. G. Roux, E. Levêque, N. Mordant, J.-F. Pinton, and A. Arneodo. Lagrangian velocity statistics in turbulent flows: Effects of dissipation. *Physical Review Letters*, 91(21), Nov 2003.

[22] A. Chorin. *Vorticity and Turbulence*. Springer, Berlin, 1994.

[23] P. Constantin and G. Iyer. A stochastic lagrangian representation of the three- dimensional incompressible navier–stokes equations. *Comm. Pure Appl. Math*, LXI:0330–0345, 2008.

[24] A. M. Crawford, N. Mordant, and E. Bodenschatz. Joint statistics of the lagrangian acceleration and velocity in fully developed turbulence. *Physical Review Letter*, 94(2):024501, 2005.

[25] S. Douady, Y. Couder, and M. E. Brachet. Direct observation of the intermittency of intense vorticity filaments in turbulence. *Phys. Rev. Lett.*, 67:983–986, Aug 1991.

[26] T. D. Drivas. Turbulent cascade direction and lagrangian time-asymmetry. *Journal of Nonlinear Science*, 29(1):65–88, 2019.

[27] B. Dubrulle. Beyond kolmogorov cascades. *Journal of Fluid Mechanics*, 867, mar 2019.

[28] G. Falkovich, H. Xu, A. Pumir, E. Bodenschatz, L. Biferale, G. Boffetta, A. S. Lanotte, and F. Toschi. On lagrangian single-particle statistics. *Physics of Fluids*, 24(5):055102, 2012.

[29] Y. Gagne and B. Castaing. Une representation universelle sans invariance globale d'échelle des spectres d'énergie en turbulence développée. *CR. Acad. Sci.*, 312(serie 2):441–445, 1991.

[30] C. W Gardiner. *Handbook of Stochastic Methods for Physics, Chemistry and the Natural Sciences*. Springer, 1985.

[31] S. S. Girimaji and S. B. Pope. A diffusion model for velocity gradients in turbulence. *Physics of Fluids A: Fluid Dynamics*, 2(2):242–256, 1990.

[32] N. Goldenfeld. *Lectures on Phase Transitions and the Renormalization Group*. Westview press, 1992.

[33] M. Gorokhovski and R. Zamansky. Modeling the effects of small turbulent scales on the drag force for particles below and above the kolmogorov scale. *Physical Review Fluids*, 3(3):1–23, March 2018.

[34] J. F. Hackl, P. K. Yeung, and B. L. Sawford. Multi-particle and tetrad statistics in numerical simulations of turbulent relative dispersion. *Physics of Fluids*, 23(6):065103, Jun 2011.

[35] R. J. Hill. Scaling of acceleration in locally isotropic turbulence. *Journal of Fluid Mechanics*, 452:361–370, 2002.

[36] H. Homann, D. Schulz, and R. Grauer. Conditional Eulerian and Lagrangian velocity increment statistics of fully developed turbulent flow. *Physics of Fluids*, 23(5):055102, May 2011.

[37] Y. Huang and F. G. Schmitt. Lagrangian cascade in three-dimensional homogeneous and isotropic turbulence. *Journal of Fluid Mechanics*, 741, Feb 2014.

[38] A. Innocenti, N. Mordant, N. Stelzenmuller, and S. Chibbaro. Lagrangian stochastic modelling of acceleration in turbulent wall-bounded flows. *Journal of Fluid Mechanics*, 892:A38, 2020.

[39] P. L. Johnson and C. Meneveau. A closure for lagrangian velocity gradient evolution in turbulence using recent-deformation mapping of initially gaussian fields. *Journal of Fluid Mechanics*, 804:387–419, 2016.

[40] P. L. Johnson and C. Meneveau. Predicting viscous-range velocity gradient dynamics in large-eddy simulations of turbulence. *Journal of Fluid Mechanics*, 837:80–114, Dec 2017.

[41] P. L. Johnson and C. Meneveau. Restricted Euler dynamics along trajectories of small inertial particles in turbulence. *Journal of Fluid Mechanics*, 816, 2017.

[42] P. L. Johnson and C. Meneveau. Turbulence intermittency in a multiple-time-scale Navier-Stokes-based reduced model. *Physical Review Fluids*, 2(7), Jul 2017.

[43] J.-P Kahane and J Peyrière. Sur certaines martingales de Benoit Mandelbrot. *Advances in Mathematics*, 22(2):131–145, 1976.

[44] A. N. Kolmogorov. The Local Structure of Turbulence in Incompressible Viscous Fluid for Very Large Reynolds Numbers.

Dokl. Akad. Nauk SSSR, 434:9–13, 1941. Translation by V. Levin in Philosophical Transactions of The Royal Society A 1991 vol. 434 p. 9-13.

[45] A. N. Kolmogorov. On the log-normal distribution of particles sizes during break-up process. *Dokl. Akad. Nauk SSSR*, 31(99), 1941.

[46] A. N. Kolmogorov. A refinement of previous hypotheses concerning the local structure of turbulence in a viscous incompressible fluid at high Reynolds number. *Journal of Fluid Mechanics*, 13:82–85, 1962.

[47] B. Kumar, J. Schumacher, and R. A. Shaw. Lagrangian mixing dynamics at the cloudy–clear air interface. *Journal of the Atmospheric Sciences*, 71(7):2564 – 2580, 2014.

[48] A. La Porta, G. A. Voth, A. M. Crawford, J. Alexander, and E. Bodenschatz. Fluid particle accelerations in fully developed turbulence. *Nature*, 409:1017–1019, 2001.

[49] A. G. Lamorgese, S. B. Pope, P. K. Yeung, and B. L. Sawford. A conditionally cubic-Gaussian stochastic Lagrangian model for acceleration in isotropic turbulence. *Journal of Fluid Mechanics*, 582:243–448, 2007.

[50] A. Lanotte, E. Calzavarini, T. Federico, B. Jeremie, B. Luca, and C. Massimo. Heavy particles in turbulent flows. International CFD Database, 2011.

[51] A.S. Lanotte, L. Biferale, G. Boffetta, and F. Toschi. A new assessment of the second-order moment of lagrangian velocity increments in turbulence. *Journal of Turbulence*, 14(7):34–48, 2013.

[52] J. M. Lawson, E. Bodenschatz, A. N. Knutsen, J. R. Dawson, and N. A. Worth. Direct assessment of Kolmogorov's first refined similarity hypothesis. *Physical Review Fluids*, 4(2), Feb 2019.

[53] F. Le Roy De Bonneville, R. Zamansky, F. Risso, A. Boulin, and J.-F. Haquet. Numerical simulations of the agitation generated by coarse-grained bubbles moving at large reynolds number. *Journal of Fluid Mechanics*, 926:A20, 2021.

[54] R. Letournel, L. Goudenège, R. Zamansky, A. Vié, and M. Massot. Reexamining the framework for intermittency in Lagrangian stochastic models for turbulent flows: A way to an original and versatile numerical approach. *Phys. Rev. E*, 104:015104, Jul 2021.

[55] B. B. Mandelbrot. Possible refinement of the lognormal hypothesis concerning the distribution of energy dissipation in intermittent turbulence. In M. Rosenblatt and C. Van Atta, editors, *Statistical Models and Turbulence*, pages 333–351, Berlin, Heidelberg, 1972. Springer Berlin Heidelberg.

[56] B. B. Mandelbrot. Intermittent turbulence in self-similar cascades: divergence of high moments and dimension of the carrier. *Journal of Fluid Mechanics*, 62(2):331–358, 1974.

[57] C. Meneveau. Lagrangian Dynamics and Models of the Velocity Gradient Tensor in Turbulent Flows. *Annual Review of Fluid Mechanics*, 43:219–245, 2011.

[58] C. Meneveau and T. S. Lund. On the lagrangian nature of the turbulence energy cascade. *Physics of Fluids*, 6(8):2820–2825, 1994.

[59] A. S. Monin and A. M. Yaglom. *Statistical Fluid Mechanics: Mechanics of Turbulence*, volume 2. MIT Press, Cambridge, MA, 1981.

[60] N. Mordant, A. M. Crawford, and E. Bodenschatz. Experimental lagrangian acceleration probability density function measurement. *Physica D: Nonlinear Phenomena*, 193(1-4):245–251, 2004.

[61] N. Mordant, A. M. Crawford, and E. Bodenschatz. Three-dimensional structure of the lagrangian acceleration in turbulent flows. *Physical Review Letter*, 93(21):214501, 2004.

[62] N. Mordant, J. Delour, E. Lévêque, A. Arnéodo, and J.-F. Pinton. Long time correlations in lagrangian dynamics: a key to intermittency in turbulence. *Physical Review Letter*, 89(25):254502, 2002.

[63] N. Mordant, E. Lévêque, and J.-F. Pinton. Experimental and numerical study of the Lagrangian dynamics of high reynolds turbulence. *New Journal of Physics*, 6:116–116, sep 2004.

[64] A. M. Oboukhov. Some specific features of atmospheric tubulence. *Journal of Fluid Mechanics*, 13(01):77–81, 1962.

[65] R. M. Pereira, L. Moriconi, and L. Chevillard. A multifractal model for the velocity gradient dynamics in turbulent flows. *Journal of Fluid Mechanics*, 839:430–467, 2018.

[66] C. S. Peskin. A random-walk interpretation of the incompressible Navier-Stokes equations. *Communications on Pure and Applied Mathematics*, 38(6):845–852, 1985.

[67] J. R. Picardo, A. Bhatnagar, and Samriddhi S. Ray. Lagrangian irreversibility and Eulerian dissipation in fully developed turbulence. *Phys. Rev. Fluids*, 5:042601, Apr 2020.

[68] S. B. Pope. Lagrangian Microscales in Turbulence. *Philosophical Transactions of the Royal Society of London*, 333(1631):309–319, 1990.

[69] S. B. Pope. On the relationship between stochastic lagrangian models of turbulence and second-moment closures. *Physics of Fluids*, 6(2):973–985, 1994.

[70] S. B. Pope. A stochastic Lagrangian model for acceleration in turbulent flows. *Physics of Fluids*, 14(7):2360, 2002.

[71] S. B. Pope and Y. L. Chen. The velocity-dissipation probability density function model for turbulent flows. *Physics of Fluids*, 2(8):1437–1449, 1990.

[72] A. Pumir, H. Xu, G. Boffetta, G. Falkovich, and E. Bodenschatz. Redistribution of kinetic energy in turbulent flows. *Phys. Rev. X*, 4:041006, Oct 2014.

[73] A. M. Reynolds. On the application of nonextensive statistics to lagrangian turbulence. *Physics of Fluids*, 15(1):L1–L4, Jan 2003.

[74] A. M. Reynolds. Superstatistical mechanics of tracer-particle motions in turbulence. *Physical Review Letter*, 91:084503, Augparticles, turbulence 2003.

[75] A. M. Reynolds, N. Mordant, A. M. Crawford, and E. Bodenschatz. On the distribution of lagrangian accelerations in turbulent flows. *New Journal of Physics*, 7(1):58, 2005.

[76] A. M. Reynolds, K. Yeo, and C. Lee. Anisotropy of acceleration in turbulent flows. 70(1), 2004.

[77] A.M Reynolds. Superstatistical lagrangian stochastic modeling. *Physica A: Statistical Mechanics and its Applications*, 340(1):298 – 308, 2004. News and Expectations in Thermostatistics.

[78] V. Sabel'nikov, A. Chtab-Desportes, and M. Gorokhovski. New sub-grid stochastic acceleration model in LES of high-Reynolds-number flows. *European Physical Journal B*, 80(2):177–187, 2011.

[79] Vladimir Sabelnikov, Alexis Barge, and Mikhael Gorokhovski. Stochastic modeling of fluid acceleration on residual scales and dynamics of suspended inertial particles in turbulence. *Phys. Rev. Fluids*, 4(4):044301, 2019.

[80] B. L. Sawford. Reynolds number effects in Lagrangian stochastic models of turbulent dispersion. *Physics of Fluids A: Fluid Dynamics*, 3:1577, 1991.

[81] B. L. Sawford and P. K. Yeung. Kolmogorov similarity scaling for one-particle Lagrangian statistics. *Physics of Fluids*, 23(9):091704, 2011.

[82] B. L. Sawford and P. K. Yeung. Turbulent lagrangian velocity statistics conditioned on extreme values of dissipation. *Procedia IUTAM*, 9:129–137, 2013. IUTAM Symposium on Understanding Common Aspects of Extreme Events in Fluids.

[83] B. L. Sawford and P. K. Yeung. Direct numerical simulation studies of Lagrangian intermittency in turbulence. *Phys. Fluids*, 27:065109, 2015.

[84] B. L. Sawford, P. K. Yeung, M. S. Borgas, P. Vedula, A. La Porta, A. M. Crawford, and E. Bodenschatz. Conditional and unconditional acceleration statistics in turbulence. *Physics of Fluids*, 15(11):3478–3489, 2003.

[85] S. Tang, R. Antonia, L. Djenidi, and Y. Zhou. Scaling of the turbulent energy dissipation correlation function. *Journal of Fluid Mechanics*, 891:A26, 2020.

[86] H. Tennekes. Eulerian and lagrangian time microscales in isotropic turbulence. *Journal of Fluid Mechanics*, 67(3):561–567, 1975.

[87] H. Tennekes and J. L. Lumley. *A First Course in Turbulence*. MIT Press, 1972.

[88] B. Viggiano, J. Friedrich, R. Volk, M. Bourgoin, R. B. Cal, and L. Chevillard. Modelling Lagrangian velocity and acceleration in turbulent flows as infinitely differentiable stochastic processes. *Journal of Fluid Mechanics*, 900:A27, 2020.

[89] G.A. Voth, A. La Porta, A.M. Grawford, J. Alexander, and E. Bodenschatz. Measurements of particle accelerations in fully developed turbulence. *Journal of Fluid Mechanics*, 469:121, 2002.

[90] Michael Wilkinson and Alain Pumir. Spherical ornstein-uhlenbeck processes. *J Stat Phys*, 145:113–142, 2011.

[91] H. Xu, A. Pumir, G. Falkovich, E. Bodenschatz, M. Shats, H. Xia, N. Francois, and G. Boffetta. Flight–crash events in turbulence. *Proceedings of the National Academy of Sciences*, 111(21):7558–7563, 2014.

[92] A. M. Yaglom. The Influence of Fluctuations in Energy Dissipation on the Shape of Turbulence Characteristics in the Inertial Interval. *Soviet Physics Doklady*, 11:26, July 1966.

[93] A. Yakhot, S. A. Orszag, V. Yakhot, and M. Israeli. Renormalization Group Formulation of Large-Eddy Simulations. *Journal of Scientific Computing*, 4(2):139–158, 1989.

[94] P. K. Yeung, S. B. Pope, A. G. Lamorgese, and D. A. Donzis. Acceleration and dissipation statistics of numerically simulated isotropic turbulence. *Physics of Fluids*, 18:065103, 2006.

[95] R. Zamansky, F. Coletti, M. Massot, and A. Mani. Turbulent thermal convection driven by heated inertial particles. *Journal of Fluid Mechanics*, 809:390–437, 2016.

[96] R. Zamansky, I. Vinkovic, and M. Gorokhovski. Acceleration in turbulent channel flow: universalities in statistics, subgrid stochastic models and an application. *Journal of Fluid Mechanics*, 721:627–668, 2013.

[97] Z. Zhang, D. Legendre, and R. Zamansky. Model for the dynamics of micro-bubbles in high reynolds number flows. *Journal of Fluid Mechanics*, 879:554–578, 2019.